Hf-Nd input flux in the Izu-Mariana subduction zone and recycling of subducted material in the mantle

Catherine Chauvel and Jean-Christophe Marini

LGCA,CNRS, Université Joseph Fourier, BP 53, F-38041 Grenoble Cedex 09, France (catherine.chauvel@ujf-grenoble.fr)

Terry Plank

Department of Earth Sciences, Boston University, 685 Commonwealth Ave., Boston, Massachusetts 02215, USA

Now at: Lamont Doherty Earth Observatory and Department of Earth and Environmental Sciences, Columbia University, PO Box 1000, Palisades, NY 10964, USA (tplank@ldeo.columbia.edu)

John N. Ludden

British Geological Survey, Keyworth, Nottingham, UK (jludden@bgs.ac.uk)

Abstract

In subduction zones, two major mass fluxes compete: the input flux of altered oceanic crust and sediments subducted into the mantle and the output flux of magma that forms the volcanic arc. While the composition and the amount of material erupted along volcanic arcs are relatively well known, the chemical and isotopic composition of the subducted material (altered oceanic crust and sediments) is poorly constrained and is an important factor in the mass balance calculation. ODP Leg 185 in the Western Pacific used systematic sampling of the altered basaltic basement and sediment pile and the creation of composite mixtures to quantify the total chemical flux subducted at the Izu-Mariana margin. Here, we report Hf and Nd isotopic compositions of materials recovered from this Leg. The Hf and Nd isotopic compositions of altered basalts from Hole 801C are indistinguishable from those of recent unaltered Pacific MORB suggesting that hydrothermal alteration had no effect on either isotopic systems.

The complete Site 1149 sedimentary pile has a weighted average ε_{Nd} of –5.9 and ε_{Hf} of +4.4, values similar to those of Fe-Mn crusts and nodules. Therefore, the Hf and Nd isotopic compositions of the sediments collected at Site 1149 indicate minimal contributions from continental detrital material to the REE and HFSE. However, the Hf isotopic budget of the oldest sediments is more influenced by continental material than the younger sediments, despite the large distances to continental masses 130 Ma ago.

In the Izu subduction zone, we calculate a sedimentary input of less than about 2% in the volcanic lava source. In contrast, at least 85% of the sedimentary Nd and Hf are recycled into the mantle to affect its general composition. Assuming that sediments have been recycled in a similar manner into the mantle for millions of years, large chemical heterogeneities must be produced in the mantle. In addition, the depletion

of the mantle due to the extraction of continental crust must be partly counterbalanced by the injection of vast quantities of enriched sedimentary material.

Introduction

Subduction zones are the principal sites for exchange between the mantle and surficial geochemical reservoirs: the crust, ocean and atmosphere. Magmas from subduction zones contribute to crustal growth and deliver volatile elements to the atmosphere. In return, the mantle is fertilized by subduction of altered oceanic crust and sediments containing elements derived from the continental crust and seawater (Armstrong, 1968; Armstrong, 1991; VonHuene and Scholl, 1991; VonHuene and Scholl, 1993; Plank and Langmuir, 1998) .

Quantifying fluxes between material entering the subduction zone and volcanic outputs requires, on one hand, an accurate estimate of the chemical and isotopic composition of arc magmas and, on the other hand, a precise evaluation of the chemical and isotopic composition of subducted materials. Such evaluations have been made on a global scale by Plank and Langmuir (1998), who calculated average compositions for sediments subducted under various arcs as well as a global sediment composition called GLOSS. However, no complete section of basaltic crust and overlying sediments had ever been studied for its complete trace element and isotopic compositions. The primary scientific objective of ODP Leg 185, which was drilled in 1999 in the western Pacific, outboard of the Izu-Bonin-Mariana arc, was to sample and characterize a complete section of altered basaltic crust and overlying sedimentary pile (Plank et al., 2000). Altered basaltic crust was drilled at Hole 801C, east of the Mariana arc, and the sedimentary pile and basaltic basement were sampled at Site 1149 in front of the Izu arc. As part of this joint international effort, we analyzed Nd and Hf isotopes of basaltic samples from Hole 801C and sediments collected at Site 1149 while other teams concentrated their efforts on the mobility of trace elements in the basaltic basement (Kelley et al., 2003; Reisberg et al., 2008), on the Sr, Nd, Pb isotopic systematics of both sediments and basalts (Hauff et al., 2003),

or on the trace element budget of the entire sedimentary pile (Plank et al., 2007). Comparing the Nd and Hf isotopic compositions of the old altered basaltic crust with those of fresh Pacific MORB should provide constraints on the behavior of rare earth elements (REE) and high field strength elements (HFSE) during alteration of oceanic crust. These data will also provide a composition for oceanic crust recycled into the mantle. In addition, Nd and Hf isotopic compositions measured on the Site 1149 sediments provide constraints on the origin of REE and HFSE in sediments deposited in ocean basins, and can be used to evaluate the average composition of downgoing sedimentary material in intra-oceanic subduction zones. Our sediment results may also be compared to the pioneering Hf isotopic work on sediments from the western Pacific area of Woodhead (1989) and Pearce et al. (1999).

Our work constrains the composition of the subducted materials regionally, and can be used to understand the genesis of the Izu-Mariana arc lavas. Western Pacific arcs have been exceptionally well studied, particularly for Nd and Hf isotopes (White and Patchett, 1984; Woodhead, 1989; Elliott et al., 1997; Pearce et al., 1999; Woodhead et al., 2001; Tollstrup and Gill, 2005; Wade et al., 2005; Stern et al., 2006). In spite of this, there are no good estimates of the Nd-Hf input flux to these arc systems. More generally, such data on a complete section of subducted material provides an estimate of the flux of chemical elements recycled into the mantle and can help in understanding the long term evolution of the composition of the mantle as a result of the balance between melt extraction through volcanic activities, and recycling of basaltic crust and overlying sediments in subduction zones.

Sample selection

We focused our study on two different sets of samples: the first set is the suite of composite samples of basalts prepared by Kelley et al. (2003) to characterize the

basaltic crust entering the subduction zone and sampled at ODP Site 801C (see Figure 1). This is the oldest crust formed at fast spreading rates, and so is the reference basement section for much of the subducting western Pacific oceanic crust (Ludden et al., 2006). The second set is a selection of sediment samples from ODP Site 1149 which represent the sedimentary cover overlying the oceanic crust (Figure 1). This site reflects all the major types of pelagic sedimentation found in the western Pacific, including chert, clay, and carbonate lithologies (Plank et al., 2007). Samples were selected to cover the entire variability of the basaltic and sedimentary compositions along the cores and once weight averaged, they should represent the average composition of the old Pacific plate that enters subduction zones along a large sector of the western Pacific convergent margin.

- *The basaltic basement drilled at ODP Site 801C*

Hole 801C (18°38.5'N, 156°21.6'E) is located in the Pigafetta Basin (Figure 1), 950 km east of the Mariana trench. This hole was first drilled in 1989 during ODP Leg 129 (Lancelot et al., 1990). In 1999 during ODP Leg 185, the hole was deepened to collect a more complete section of the altered oceanic crust (Plank et al., 2000). A total thickness of 474 m was sampled and divided into eight major sequences based on petrological, mineralogical and geochemical characteristics. The uppermost sequence consists of alkalic basalts and dolerites (about 20m thick) while lower sequences are typical MORB with tholeiitic composition including massive flows or pillows associated with breccias, volcanoclastic material and silicic hydrothermal deposits (Plank et al., 2000; Barr et al., 2002; Fisk and Kelley, 2002). The upper alkalic basalts have an Ar-Ar age of 157 Ma and the underlying MORB have ages ranging from 162 to 171 Ma (Pringle, 1992; Koppers et al., 2003a). Most basaltic materials from hole 801C are altered by low temperature hydrothermal fluids and interaction with low-temperature seawater, and the material varies from highly altered

interpillow materials to better preserved massive flows. Some completely unaltered volcanic glasses also exist (Alt et al., 1992; Plank et al., 2000; Fisk and Kelley, 2002; Talbi and Honnorez, 2003).

A set of composite samples was prepared by mixing powders of the various lithologies (massive flows, pillows, breccias, volcanoclastic materials and hydrothermal deposits) according to their respective proportions in the hole. The procedure followed for sample preparation, as given by Kelley et al. (2003) led to the preparation of thirteen composites representing the flows and pillows units, the breccias and volcanoclastic sediments. A global composite representative of the entire basaltic column was also prepared. Major and trace element compositions of these composites were measured by Kelley et al. (2003), stable isotopes have been published by Alt (2003) and Re-Os results were reported by Reisberg et al. (2008). Our Hf and Nd isotopic compositions were obtained on the same composite samples.

- *The sedimentary pile drilled at ODP Site 1149*

The sedimentary cover subducted at the Mariana trench has been drilled and sampled during several DSDP and ODP campaigns (especially during the ODP Leg 129) and is one of the best studied sedimentary piles on a subducting oceanic plate (Plank and Langmuir, 1998). In contrast, the sedimentary pile subducted in the Izu-Bonin region, north of the Mariana arc, was largely unknown and was therefore drilled at Site 1149 during ODP leg 185 (31°20.1'N, 143°21.8'E see Figure 1).

In the Izu-Bonin region the sediments covering the Pacific crust have a thickness of about 410 m and include several lithological units (figure 2):

-Unit I, at the top of the sediment pile, has a thickness of about 118 m. It consists of a mixture of clay minerals, siliceous planktonic microfossils (essentially

diatoms and radiolarians) and volcanic ash. Paleomagnetic data indicate an age from late Miocene (about 6.5 Ma) to late Pleistocene (younger than 0.2 Ma).

-Unit II (including subunits IIA and IIB) has a thickness of about 62 m, and consists almost exclusively of pelagic clays. However, in the upper part, defined as subunit IIA, some ash layers are present. The lowest part of unit II, called subunit IIB, is entirely composed of pelagic clays. The transition between subunit IIB and unit III is marked by the presence of zeolitic clays. The ages within unit II remain unknown by lack of paleomagnetic or biostratigraphic data but the unit reflects most of the age history of the site (from 6.6 Ma to 105 Ma (Plank et al., 2007)).

-Unit III mainly consists of biogenic siliceous deposits: radiolarian cherts and radiolarian porcelanite. Some claystones were also recovered, essentially in the uppermost and in the lowest part of the unit. The thickness of unit III is about 103 m and its deposition age ranges from 105 to 127 Ma (Plank et al., 2007).

-Unit IV has a thickness of 126 m and is characterized by a mixture of radiolarian cherts and porcelanite with calcareous sediments (marlstone and chalk). An isolated ash-rich level is also present at the top of the unit. Nannofossils preserved in marls and chalks indicate a late Valanginian (134 Ma) to late Hauterivian (127 Ma) age for this unit.

Discrete samples were selected along the entire Site 1149 sedimentary column from unit I to unit IV (Plank et al., 2000). Their major and trace element compositions were measured by Plank et al. (2007) and we report here Hf and Nd isotopic compositions on a selection of this sediment set. Eighteen samples from the various lithologies were selected in the different units to cover the entire compositional spectrum. This same subset of samples have been studied by several investigators, and so together, form a remarkably complete data set for elemental and isotopic compositions (Ludden

et al., 2006; Plank et al., 2007). The measured Hf and Nd isotopic variations should therefore be representative of the entire sedimentary pile.

Analytical Procedure

Hf and Nd chemical separation were performed in Grenoble and the isotopic compositions were measured using the VG Plasma 54 at ENS Lyon. Samples were dissolved in Savillex beakers but dissolution in Parr bombs were also performed on selected samples to check that complete dissolution of the sediments was achieved (see Table 2). The analytical procedure for Hf separation was based on the method published by Blichert-Toft et al. (1997) which proved to be highly efficient for most of the Site 801C composites and Site 1149 sediments, but this method failed for two particular sample groups (cherts and Ca-rich sediments) and had to be modified. Detailed suggestions relative to the isolation of Hf for these two groups of sediments are given in the appendix. Nd was isolated from the other REE using the classical Eichrom® HDEHP-coated teflon resin technique. Hf and Nd blanks were measured regularly by ICP-MS and were always lower than 80 pg for Hf and 235 pg for Nd; these values are negligible relative to the amounts of Hf and Nd present in the samples.

Accuracy of the isotopic measurements was monitored on the P54 at ENS Lyon using the JMC-475 Hf standard. The average measured $^{176}Hf/^{177}Hf$ ratio was 0.282163±11 (1σ, 32 runs). Two different standards were used during Nd analysis: an internal "home" Nd JMC standard which gave an average $^{143}Nd/^{144}Nd$ ratio of 0.512238±7 (1σ, 12 runs) and the Nd La Jolla standard which gave an average $^{143}Nd/^{144}Nd$ ratio of 0.511858±10 (1σ, 8 runs). Several complete duplicate analyses were performed and results show that for both Nd and Hf isotopic ratios, the measurements reproduce within analytical errors ($\leq 1\varepsilon_{Nd}$ or ε_{Hf}) (see Tables 1 and 2).

Results

- *Site 801C basalt composites*

Hf and Nd isotopic compositions of Hole 801C composites are reported in Table 1 together with calculated present-day and initial ε_{Hf} and ε_{Nd} values. The lithology of each composite is also indicated in the footnote. The measured and initial Hf and Nd isotopic compositions of Hole 801C samples are plotted in Figure 3 together with values for present-day mid-ocean ridge basalts (MORB) and oceanic island basalts (OIB). This figure shows that the MORB composites have Hf and Nd isotopes indistinguishable from those of present day Pacific MORB. The three alkali basalt composites have very different isotopic compositions and plot in the OIB field close to some of the Austral HIMU samples. When compared to the four samples from site 801 (2 MORB and 2 OIB) analyzed by Pearce et al. (1999), a slight discrepancy is observed (see Figure 3): while the initial ε_{Hf} are comparable, our analyses are systematically lower for Nd. The origin of the discrepancy is unclear because our Nd La Jolla measurements are similar to the value mentioned by Pearce et al. (1999).

- *Site 1149 sediments*

The measured Hf and Nd isotopic ratios for Site 1149 sediments are reported in Table 2. Initial ε_{Hf} and ε_{Nd} values were also calculated using paleomagnetic and biostratigraphic ages (Bartolini, 2003) for samples from units I, III and IV. For units IIA and IIB, ages are unknown by lack of magnetostratigraphic or biostratigraphic record. However, the sedimentation rate was particularly slow during deposition of these units, at about 1 m/Ma if calculated over the entire time period and it does not seem to have varied through time. The initial Hf and Nd isotopic compositions of

229 samples from units IIA and IIB were therefore calculated using this sedimentation rate
230 and the depth at which samples occur.
231 The initial ε_{Hf} and ε_{Nd} of all samples are plotted along the sedimentary column in
232 Figure 4. $\varepsilon_{Nd(i)}$ values define a limited range between –8 and –5 with three exceptions,
233 two samples from Unit I and one sample from Unit IV, which all have significantly
234 more radiogenic Nd isotopic compositions (–3 to –1.6). Hauff et al. (2003) also
235 reported Nd isotopic compositions obtained on samples from the same Leg and eight
236 of our samples were also measured by them for Nd, Sr and Pb isotopes. Reported
237 values are in excellent agreement and the difference between our values and those
238 reported by Hauff et al. (2003) is always smaller than 50 ppm.
239 Hf isotopes do not define the same pattern as Nd isotopes: while sediments from the
240 top of the column have positive $\varepsilon_{Hf(i)}$ values at about +6, samples from the bottom of
241 the pile have negative $\varepsilon_{Hf(i)}$ values at about –5, and the change occurs gradually
242 through time. Two samples from the bottom of the pile and one sample from the top
243 of the pile do not follow the general trend and have significantly more positive $\varepsilon_{Hf(i)}$ at
244 +10.3, +8 and +12 (see Table 2 and Figure 4). When plotted in a $\varepsilon_{Hf(i)}$ vs. $\varepsilon_{Nd(i)}$
245 diagram (Figure 5), the Site 1149 sediments can be compared to the various types of
246 oceanic sediments that have been published in the literature. This figure shows that
247 almost all Site 1149 sediments plot in the Fe-Mn crusts and nodule field, above the
248 “terrestrial array” defined by Vervoort et al. (1999). In addition, the progressive
249 increase through time of $\varepsilon_{Hf(i)}$ at constant $\varepsilon_{Nd(i)}$ appears clearly: samples from unit IV
250 are located next to the terrestrial array while samples from unit I have the most
251 radiogenic Hf isotopes. Four exceptions exist, samples 7H4 and 10H3 from unit I and
252 samples 16R1 and 29R1 from unit IV which have distinctively higher $\varepsilon_{Hf(i)}$ or $\varepsilon_{Nd(i)}$
253 values and do not plot along the general sub-vertical trend (Figure 5).
254

Discussion

-A- COMPOSITION OF THE SUBDUCTED PILE

- *The basalt composites*

In Site 801C, two volcanic sequences are distinguished, a thick pile of tholeiites overlain by a thin upper layer of more alkaline lavas. Composites of the tholeiitic rocks were prepared according to their depth along the drill core and according to the rock types (Kelley et al., 2003). Suffixes on the sample name in Table 1 indicate the depth range mixed in the composite while the type of material is indicated as being flows (FLO), volcaniclastics (VCL) or a mixture of the two (ALL). In addition, a composite representative of the entire tholeiitic section was prepared and called 801 SUPER. All composites have near constant Hf and Nd isotopic compositions (see Figure 3) with ε_{Hf} and ε_{Nd} values similar to those of present-day Pacific MORB (Chauvel and Blichert-Toft, 2001), suggesting that the oceanic crust created about 167 Ma ago (Pringle, 1992) originated from a mantle source equivalent to the present one. In addition, the similarity between this old Pacific oceanic crust and the basalts accreting today at the ridge suggests that alteration processes occurring after basalt formation at the ridge and during the 167 Ma of presence at the bottom of the Pacific ocean did not affect the Nd and Hf isotopes. In detail, small isotopic variations exist but no systematic trend can be found. In particular, no change occurs between composites from the upper, middle and lower part of the hole; in contrast, small but maybe systematic differences may exist between flow composites and volcaniclastic composites in terms of Hf isotopes alone with slightly more radiogenic values in the volcaniclastics than in the flows. However, the difference is so small that it might be an artifact due to the limited number of analyzed samples (see Table 1).

The top alkali basalt composites (TAB in Table 1) have $\varepsilon_{Hf(i)}$ and $\varepsilon_{Nd(i)}$ values lower than the tholeiitic composites and plot in the OIB field in Figure 3 close to data

281 reported for two Jurassic OIB samples drilled at Site 801 and analyzed by Pearce et al.
282 (1999) and close to Rurutu and Raevavae, two islands in the Austral chain in
283 Polynesia (Chauvel et al., 1992; Chauvel et al., 1997; Lassiter et al., 2004; Pfänder et
284 al., 2007) confirming the OIB characteristics suggested by previous studies (Castillo
285 et al., 1992; Floyd and Castillo, 1992; Hauff et al., 2003). In addition, the strong
286 similarity between the Hf-Nd isotopic compositions of the alkali basalt composites
287 and those of Rurutu and Raevavae supports Koppers et al. (2003b) reconstruction of
288 the past history of the Austral HIMU hotspot in the Western Pacific.
289 The unmodified initial Hf and Nd isotopic compositions of Site 801C tholeiitic
290 composites together with the preserved isotopes of the alkali composites demonstrate
291 that, when considered on the bulk scale of the crust, the overall Hf and Nd isotopic
292 budget of altered basalts remains unchanged during hydrothermal and low
293 temperature alteration processes. This result extends to the Hf isotopic system the
294 conclusions reached in previous studies by Staudigel et al. (1995) who demonstrated
295 that provided samples are large enough to represent the whole rock (1-10 cm), Nd
296 isotopes of ocean basalts were not modified by hydrothermal alteration.
297

298 • *The sedimentary column*

299 With the exception of four samples discussed later, the sediments sampled at Site
300 1149 have initial Nd isotopic compositions that, irrespective of their lithology and
301 age, remain remarkably constant during the entire sedimentation history ($\varepsilon_{Nd(i)}$ vary
302 only between –6.6 and –4, see Table 2 and Figure 4). In contrast, their initial ε_{Hf}
303 values increase systematically through time: the oldest sediments from Unit IV have
304 the lowest $\varepsilon_{Hf(i)}$ values at -5 while the most recent sediments from Unit I have positive
305 $\varepsilon_{Hf(i)}$ values above +5 (Figure 4). When combined in Figure 5, data points for the
306 entire sediment pile fall in the field defined by the Fe-Mn crusts and nodules (Godfrey

et al., 1997; Albarède et al., 1998; David et al., 2001), and systematically above the terrestrial array of Vervoort et al. (1999). This suggests that during the 160 Ma of oceanic sedimentation, the Hf-Nd budget of the sediments was mainly dominated by sources with radiogenic Hf isotopes relative to their Nd isotopic compositions, as is the case with the Fe-Mn crusts and nodules, and was little influenced by direct detrital input from the continents. The reason why the older sediments register a more crustal signature than the younger sediments is unclear. Units III and IV are particularly poor in Hf and other trace elements due to the overwhelming presence of cherts and biogenic carbonates (Plank et al., 2007), while Units I and II contain a significant proportion of clays. The low ε_{Hf} values of the older sediments are therefore not associated to a high proportion of silicates coming from a continental source. In addition, 130 Ma ago, the sediments were deposited far away from any continent, in the middle of the gigantic Pacific superocean (Bartolini and Larson, 2001).

There are four exceptions to this general trend: samples 29R1 and 16R1 from unit IV and samples 7H4 and 10H3 from unit I. Sample 29R1 is a calcareous marl located few centimeters above the basaltic basement. Plank et al. (2000; 2007) noticed that the lowermost sediments contain significant enrichments in metalliferous elements such as Mn and Fe and these sediments were interpreted as resulting from the presence of hydrothermal vents. While the Nd isotopic composition reported by Hauff et al. (2003) for sample 29R1 is similar to that of other samples, its Sr and Pb isotopic ratios are lower than in other samples. Our measured Hf isotopic composition for sample 29R1 is extremely radiogenic and approaches values obtained on the Site 801 basaltic basement. We suggest therefore that the Hf isotopic value reported for this sample is strongly influenced by the underlying basaltic crust, most likely due to hydrothermal sedimentation.

Sample 16R1 from Unit IV and samples 7H4 and 10H3 from Unit I contain volcanic ashes in proportions varying between 10 and 15% (Plank et al., 2007), and their position in Figure 5 to the right of the trend defined by the other samples in the sedimentary pile can easily be explained by the contribution of volcanic products to the sediment composition. Plank et al. (2000) suggested that the volcanic ash present in samples 7H4 and 10H3 from Unit I could very well come from the Western Pacific volcanic arcs such as the Izu-Bonin-Marianne arc. This suggestion is entirely consistent with (a) the Hf and Nd isotopic compositions of the two samples from Unit I, which are displaced from the sediment pile field in Figure 5 towards more radiogenic isotopic compositions, and (b) the relationship between Sm/Nd and $\varepsilon_{Nd(i)}$ values shown in Figure 6 where samples 7H4 and 10H3 fall in between the field defined by the other sediments and the field defined by the Izu-Mariana volcanics. For sample 16R1 from Unit IV, the origin of the volcanic material is more difficult to evaluate because at the time when the sediment was deposited on the ocean floor, about 125 Ma ago, it was located far from any known volcanic arc, volcanic island or continental arc (see Coffin et al. (2000) and Bartolini and Larson (2001) for paleogeographic reconstruction of the Pacific plate). However, its position in Figure 6 together with the widespread recognition of OIB-type volcanic products in this part of the Pacific at that time (Staudigel et al., 1991; Castillo et al., 1992; Floyd et al., 1992; Lees et al., 1992; Koppers et al., 2003b) suggests that the volcanic ashes probably came from an ocean island located within a few hundreds of kilometers.

Our Hf and Nd isotopic measurements can be combined with trace element analyses published by Plank et al. (2007) to quantify the average composition of the entire sedimentary pile. Using an approach similar to that of Plank and Langmuir (1998) we use discrete measurements performed on carefully selected samples representative of each lithological unit to calculate the average composition of each lithology. A global

358 average of the entire sedimentary pile was then calculated using the composition of
359 each unit composition and their relative proportion in the sediment column. Results
360 are shown in Table 3 and presented in Figure 7. The sedimentary pile drilled at Site
361 1149 was initially divided in five lithological units or subunits (see figure F17 in
362 Plank et al. (2000)). However trace element analysis (Plank et al., 2007) and Hf and
363 Nd isotopes indicate the presence of some distinctive layers within the original units:
364 (a) The transition between subunit IIB and unit III consists of 10 meters of zeolitic
365 clays highly enriched in REE compared to the rest of unit III and subunit IIB samples
366 (Plank et al., 2007). We therefore treated this REE-rich layer individually when
367 performing the average calculation.
368 (b) Samples 16R1 93-98 and 29R1 28-35 from unit IV have radiogenic Hf isotopic
369 compositions compared to the other unit IV sediments (Table 2) and were considered
370 separately for the average calculation.
371 The Site 1149 sedimentary column has an average ε_{Nd} that is negative at -5.9, but its
372 ε_{Hf} value is positive at about +4.4. In Figure 7, the combined values plot in the Fe-Mn
373 crusts and nodules field significantly above the "terrestrial array" of Vervoort et al.
374 (1999), suggesting that the REE and Hf budget for the entire history of sedimentation
375 in the Pacific was dominated by mineral phases that registered a source with elevated
376 Hf isotopes as is the case with the Fe-Mn crusts and nodules.
377 Remarkably similar ε_{Hf} and ε_{Nd} values were obtained by White et al. (1986) and
378 Woodhead (1989) who measured a composite sample from DSDP Site 452 located in
379 front of the Mariana arc (see figures 1 & 7). It is also not very different from the
380 estimated average Site 801 sediment value calculated by Wade et al. (2005). This
381 suggests that the average isotopic compositions obtained in this study represent a
382 common feature for the Western Pacific sedimentary cover. However, both at DSDP
383 Site 452 in front of the Mariana arc and at ODP Site 1149 in front of the Izu arc, the

sedimentary columns do not include much volcanoclastic sediments (Hussong et al., 1982; Plank et al., 2000) whose presence would affect the average composition of the sediment cover. In other locations such as the West Pacific ODP sites 800, 801 and 802 (see figure 1) thick volcanoclastic units are present (Lancelot et al., 1990; Lees et al., 1992) and there, the average Hf and Nd isotopic compositions would probably be different, with more radiogenic Nd and Hf isotopic values. The average Hf and Nd isotopic compositions of DSDP Site 452 and ODP Site 1149 should therefore be considered as representative of Pacific sedimentary columns dominated by pelagic sediments.

-B- RECYCLING OF THE SITE 1149 SEDIMENTS IN THE IZU-MARIANA ARC SYSTEM

The trace element and isotopic characteristics of Izu arc lavas are reported a several papers (Notsu et al., 1983; Ikeda and Yuasa, 1989; Fryer et al., 1990; Hochstaedter et al., 1990a; Hochstaedter et al., 1990b; Tatsumi et al., 1992; Taylor and Nesbitt, 1998; Ishikawa and Tera, 1999; Hochstaedter et al., 2000; Hochstaedter et al., 2001; Schmidt, 2001; Straub and Layne, 2002; Straub, 2003; Straub et al., 2004) but the number of samples analyzed for Hf isotopes is quite limited. In terms of Hf and Nd isotopic compositions, Izu lavas, together with the Mariana arc lavas, are among the most radiogenic arc lavas studied up to now (White and Patchett, 1984; Woodhead, 1989; Pearce et al., 1999; Woodhead et al., 2001; Tollstrup and Gill, 2005; Wade et al., 2005; Stern et al., 2006): their Hf and Nd isotopic characteristics are not very different from those of MORB (see Figure 8). Using our estimate of the average composition of the subducted sediments, we can evaluate the proportion of sediments involved in the genesis of the arc lavas. The composition of the mantle contaminated by the sediments is a matter of debate; it could either be Indian type MORB mantle as

suggested by Hickey-Vargas et al. (1998), Savov et al. (2006), Pearce et al. (1999) and by Woodhead et al. (2001), or Pacific type MORB mantle. Here we calculated mixing arrays using a Pacific mantle because this evaluation provides a higher proportion of sedimentary material due to the more radiogenic Nd isotopic composition of the Pacific mantle; it is therefore the maximum possible contribution from the sedimentary pile. In addition, some of the data used to suggest that the mantle wedge has "Indian" characteristics are ambiguous. The samples from the Philippine basement analyzed by Savov et al. (2006) and by Pearce et al. (1999) plot in between the Indian and the Pacific MORB fields in Nd-Hf isotopic space (see Figure 8). Moreover, the overlap between the Philippine plate and the Indian MORB as shown by Hickey-Vargas et al. (1998) and by Savov et al. (2006) is accentuated by using initial ratios of the 45 Ma volcanics vs. present-day isotopic ratios for MORB. The age correction has a significant impact on the $^{206}Pb/^{204}Pb$ and $^{143}Nd/^{144}Nd$ ratios, but not on the $^{207}Pb/^{204}Pb$, $^{208}Pb/^{204}Pb$ and $^{176}Hf/^{177}Hf$ ratios. When the measured ratios are compared to the present-day MORB fields, data plot at an ambiguous intermediate position. Thus, while mantle of Indian affinity may have generated some Philippine basement, its distribution beneath the modern arcs is unknown, and given the subtle shifts in Nd and Hf that have been observed even in these "Indian" provinces, we chose the more extreme Pacific end-member to provide maximum sediment contributions.

Mixing arrays between the average subducted sediments and Pacific mantle are calculated using end-member compositions given in the caption of Figure 8 and shown in Figure 8. They fit well the data reported for both Izu and Mariana arc lavas and suggest that less than 2% of sediment mixed with depleted mantle can reproduce the island arc Hf-Nd isotopic array. This figure is very similar to the proportion of sediment suggested by Wade et al. (2005) for the Mariana arc and it is consistent with

estimates based on other trace elements or isotopic systems (i.e., (Tera et al., 1986; Ryan and Langmuir, 1988; Woodhead et al., 2001). If Indian type mantle were used instead of Pacific mantle composition, the proportion of sediment would be lower. The position of Site 1149 average sediment composition in the Hf-Nd isotopic space and the shape of the mixing array in Figure 8, also suggest that the displacement of the Izu-Bonin-Mariana arc lavas to the left of the 'MORB-OIB array' could be due to the composition of the subducted material and not necessarily due to changes of the Nd/Hf ratio during either dehydration or melting of the sediment component. This is consistent with the relationship between Hf isotopic compositions and the Hf/Hf* ratios shown in Figure 9a. Wade et al. (2005) showed that by using their estimate of the sediment composition combined with the depleted mantle value recommended by Salters and Stracke (2004), mixing curves did not pass through the Mariana island arc data field (see figures 9a & b). They suggested that the Hf/Hf* ratio of the depleted mantle might be too high, but also that the Nd/Hf ratio of the sediment involved in the source of the volcanic rocks had to be much higher than their sediment estimate (see Figure 9b and their figure 8). Using our estimate of the composition of the sediment pile, the discrepancy between mixing proportions given by the isotopic compositions (less than 2%, see Figure 8) and by the trace element ratios (less than 4%, see figures 9a & b) is lower, but still exists. To have similar proportions of sediments in the two figures requires a mantle wedge with a slight Hf deficiency relative to its REE content. Most of the Izu-Mariana arc lava data points can be explained by mixing of depleted mantle and bulk sediment. Significant outliers are the Izu forearc lavas (Pearce et al., 1999) which have extremely high Hf/Hf* and low Nd/Hf ratios and the Kasuga seamounts in the Mariana arc (Tollstrup and Gill, 2005) which have extremely low ε_{Hf} and Hf/Hf* values and high Nd/Hf ratios. These two datasets cannot be explained by any simple mixing relationship and require additional

462 processes to account for their arrays. Pearce et al. (1999) suggested that the elevated
463 Hf/Hf* values of the Izu protoarc lavas require a fractionation process that either
464 added Hf or removed REE from the lavas while Tollstrup and Gill (2005) argued that
465 residual rutile, zircon and monazite were necessary to explain the Kasuga seamount
466 array.
467 Even if the site 1149 sediments have trace element contents and Nd-Hf isotopic
468 compositions suggesting that simple bulk mixing between subducted sediments and
469 mantle wedge could explain the Nd-Hf characteristics of the Izu-Mariana island arc
470 lavas, things are more complex when other isotopic systems are considered. In
471 particular, previous studies done by Elliot et al. (1997), Ishikawa and Tera (1999),
472 Hochstaedter et al. (2001), Hauff et al. (2003) and by Straub et al. (2004) clearly
473 demonstrated that some elements were transferred from the subducted material to the
474 source of volcanics through fluid phases. Fractionation of trace elements like the
475 REE and the HFSE by residual minerals during magma genesis is also required by
476 the composition of both the Izu protoarc volcanics and the Kasuga seamounts in the
477 Mariana arc (see figures 9a & b).
478 When site 1149 data are used as the sediment contaminant in the mantle wedge below
479 the Izu arc, the modeling is quite satisfactory but the number of Nd-Hf isotopic
480 analyses on the Izu volcanics is so low that the constraints are relatively weak. More
481 analyses of the Izu volcanics would certainly help refine the general model. In the
482 case of the Mariana arc, for which a significant number of Nd-Hf analyses has been
483 published, the composition of the subducted sediment is poorly constrained: the
484 estimate suggested by Wade et al. (2005) for Site 801 has an ε_{Hf} and a Nd/Hf ratio
485 that are too low to define a mixing array going through the arc data (see figures 8 and
486 9). The Site 452 clay composite analyzed by Woodhead (1989) has ε_{Hf} and ε_{Nd} similar
487 to the Site 1149 average values (Figure 8) but no trace element data have been

488 published. Finally, the Site 1149 sediments have trace element and isotopic
489 compositions defining mixing arrays compatible with the Mariana arc data, but the
490 drill site is not located in front of the Mariana arc, and contains different sedimentary
491 units than found there (Plank et al., 2007). The main difference between the Site 1149
492 and Site 801 sedimentary averages are the Cretaceous volcaniclastics that are a major
493 part of the sedimentary input to the Marianas trench. These have isotopic
494 compositions similar to OIB, and their inclusion in the Site 801 average is responsible
495 for the lower ε_{Hf} and Nd/Hf, and the misfits to the mixing lines. One possible solution
496 to the mixing problem is that Nd and Hf are retained in the volcaniclastic unit, by the
497 preferential stability of zircon and REE phases expected in these Zr- and REE-
498 enriched materials (Klimm et al., 2008). Another possibility is simply that more data
499 are necessary to establish whether a geographical variability exists. The average
500 compositions of the subducted sediment pile in front of the Mariana arc and the Izu-
501 Bonin arc could then be compared and a well constrained model could be developed.
502 In 2003, Straub published an overview of the temporal changes in the chemical
503 composition of the Izu Bonin–Mariana arc lavas (Straub, 2003). She demonstrated
504 that over the past 50 Ma, the lava composition changed from boninitic to tholeiitic
505 with an accompanying increase in TiO_2 contents and ε_{Nd} values. Because the Nd
506 isotopic composition of the sedimentary pile is quite uniform at $\varepsilon_{Nd} \approx -6.5$ (see Table
507 2 and Figure 4), secular changes in the sediment composition cannot explain the
508 variation observed in the arc lavas. We suggest therefore that the increasingly
509 depleted nature of the arc lavas might relate to a decreasing contribution of the
510 sediment component through time.
511
512 **-C- RECYCLING OF SEDIMENTS IN ISLAND ARCS AND IN THE MANTLE**

- *Oceanic sediments and worldwide arc systems*

In more general terms, the Nd and Hf isotopic compositions of oceanic sediments can be compared to the arc lava isotopic array to evaluate their impact on the island arc compositions. In Figure 10, we show a compilation of available data published on island arcs. Not only do the data define an array that is significantly displaced to the left of the MORB-OIB array, but it also has a shallower slope: $\varepsilon_{Hf} = 1.23.\varepsilon_{Nd} +6.36$ *vs.* $\varepsilon_{Hf} = 1.59.\varepsilon_{Nd}+1.28$. While these values are slightly different from those published by Vervoort et al. (1999) mainly because of new data published within the last 10 years, they confirm the distinctive trend of arc volcanism relative to intra-plate volcanism. It can be argued, as is done by Pearce et al. (1999) and by Tollstrup (2005) that the slope of the "island arc array" results of a decoupling of Nd and Hf during dehydration and/or melting of the subducted slab with a sedimentary component characterized by elevated Nd/Hf ratios. However, we would like to suggest here that the "island arc array" could also be mainly controlled by the mixing of depleted mantle and subducted sediments. In Figure 10, we show mixing arrays between various sedimentary end-members and an average depleted mantle source. Contaminating the mantle wedge with the Leg 185 average sediment produces an array shown with a black striped line in Figure 10 that goes through the arc data with the highest ε_{Hf} values but does not appear to be the best endmember to account for the composition of most island arcs even though it can explain some arcs data (e.g., Izu, Mariana and some of the Luzon arc data). Most arc lavas lie below this mixing line with the arcs located next to continents (the Lesser Antilles and the Aegean arc) defining the lower part of the arc array. We suggest therefore that depending on the nature of the subducted sediments (sands next to continental platforms, and clays, muds and Fe-Mn crusts further away from continental margins) a range of mixing lines can be calculated. In Figure 10, we show two end-member mixing lines

539 calculated using the Nd and Hf concentrations and Nd isotopic composition of
540 GLOSS (Plank and Langmuir, 1998) for which no Hf isotopic composition is
541 available. We therefore used a range of Hf isotopic compositions as shown by the
542 vertical brown line in Figure 10. The mixing line between depleted mantle and the
543 low ε_{Hf} sand end-member reproduces well the Lesser Antilles and Aegean arcs
544 compositions while mixtures of mantle wedge and high ε_{Hf} sediments reproduce the
545 compositions of arcs such as Luzon and Sunda. In most cases, the proportion of
546 sediments involved in the source of arc volcanism is lower than 5% if straight bulk
547 mixing between sediments and mantle is used. If the sediment component is extracted
548 from the sedimentary material by either a fluid phase or a melt, the proportion of
549 sediment will be lower. We realize that this mixing model is quite simplistic and that
550 a better knowledge of the oceanic sediment compositions is really necessary. As
551 mentioned by Plank and van Keken (2008), the diversity of ε_{Hf}, ε_{Nd} and associated
552 REE/HFSE ratios in oceanic sediments needs to be better documented to understand
553 the way sediments are involved in the arc genesis.
554

555 • *Proportions of the incoming sediment flux injected back into the mantle*

556 Our average composition of the Site 1149 sedimentary pile can be used in conjunction
557 with physical and chemical data to estimate the fraction of subducted sediments that is
558 transferred directly into the arc system, and the fraction that is sent back into the
559 convecting mantle.
560 The sediment input flux can be evaluated using the convergence rate of the Pacific
561 plate, the thickness of the sediment pile, and its density, water content and average Nd
562 and Hf concentrations. All these values, which are summarized in Table 4, allow
563 estimates of the Nd input flux from the sediment at 857 kg/km of arc/yr and of the Hf
564 input rate at 49 kg/km of arc/yr. The volcanic arc output flux can be evaluated using

565 the magmatic addition rates determined by Dimalanta et al. (2002) for the Izu-Bonin
566 arc and the average Nd and Hf concentrations of arc lavas (White and Patchett, 1984;
567 Pearce et al., 1999). Using the values listed in Table 4, we calculate a Nd output rate
568 of about 1375 kg/km of arc/yr and a Hf output rate of about 312 kg/km of arc/yr. The
569 Nd and Hf present in the arc lavas originate most probably from both the mantle
570 wedge and the subducted material. Using the ε_{Nd} values given in Table 4 for the
571 average arc lavas, the mantle wedge and the subducted material, we can calculate that
572 about 10% ± 6% of the Nd present in the arc lavas comes from the subducted
573 sediment, i.e., 138 ± 82 kg/km of arc/yr. Subtracting this amount from the total
574 amount of Nd present in the subducted sediment pile implies that about 85% ± 9% of
575 the sedimentary Nd is sent back into the convecting mantle.
576 A similar calculation carried out for Hf does not provide well-constrained proportions
577 because the ε_{Hf} values of mantle wedge and arc lava are almost indistinguishable.
578 However, using the Nd/Hf ratios of the three components, we can place limits to the
579 proportion of Hf from the sediment pile that is transferred to the arc lavas and the
580 amount that is recycled into the mantle. Assuming that the sedimentary material
581 involved in the arc lava genesis has the same Nd/Hf ratio as the sediment itself, we
582 evaluate the Hf flux from sediment to arc lava as 7.9 kg/km of arc/yr and calculate
583 that 85% ± 9% of sedimentary Hf is recycled back into the mantle. It is very unlikely
584 that the Nd/Hf of the material coming out of the subducted material is lower than that
585 of the sediment because Nd is considered as more mobile in fluid phases than Hf
586 (Kogiso et al., 1997; Johnson and Plank, 1999). Dehydration products are therefore
587 likely to have a Nd/Hf $\geq$ 17.5 and transfer less than the 7.9 kg/km of arc/yr calculated
588 above. This in turn suggests that a minimum of 85% of the sedimentary Hf is
589 recycled back into the mantle.

In summary, the Nd and the Hf present in the sedimentary pile contribute to the arc lava composition but the vast majority (≥ 85%) is recycled into the mantle of the Earth to affect its general isotopic composition. Assuming that similar material has been recycled into the mantle over long periods of time during Earth history, its composition, which differs significantly from that of normal mantle, can create large chemical and isotopic heterogeneities. As already suggested by previous authors (Hofmann and White, 1982; Chauvel et al., 1992; Blichert-Toft and Albarède, 1999), such material could be present in the source of ocean island basalts. It could also be mixed into the normal depleted mantle and suppress the radiogenic growth of both Nd and Hf resulting from magmatic melt extraction of continental crust. Such modeling of the impact of recycled subducted oceanic basalt and sediments into the mantle over Earth history was performed recently by Chauvel et al. (2008) for the Nd and Hf isotopic systems and they showed that a combination of oceanic sediments and basalts could satisfactorily contribute to the mantle sources of both oceanic island basalts and mid-ocean ridge basalts and explain the "mantle array".

Conclusion

Our Hf and Nd isotopic study of the Site 1149 sediments and the Hole 801C basaltic composites leads to the following main observations:

- The similarity between Hf and Nd isotopes measured on the Site 801C basalts and present-day Pacific MORB suggest that both isotopic systems are unaffected by hydrothermal processes and low temperature alteration for a period of more than 150 Ma.

- The Hf and Nd isotopic compositions of Site 1149 sediments do not display a large range and the average composition of the entire sedimentary pile falls in the field of Fe-Mn crusts and nodules at ε_{Nd}= -5.9 and ε_{Hf} = +4.4.

- The Hf and Nd isotopic composition of the Izu-Mariana arc lavas can be modeled by mixing a Pacific type mantle wedge and less than 2% sediments and the composition of most island arc lavas can be reproduced by mixing less than 5% oceanic sediments with an ordinary depleted mantle wedge.

- We evaluate that about 85% of the Nd present in the subducted sediments is recycled into the mantle. For Hf, the proportion is constrained to be similar (85%) or higher. Consequently, most of the Nd or Hf present in the oceanic sediments is recycled into the mantle to create chemical heterogeneities and affect its average composition.

Acknowledgements

This work was financially supported by the French CNRS programs “Intérieur de la Terre” and “Dyeti”, and by the US NSF (OCE-0137110). Help in the chemistry lab provided by Francine Keller and on the Lyon MC-ICPMS by Philippe Telouk were highly valuable and discussions with Marion Carpentier, Ivan Vlastelic and Nicholas Arndt contributed to a clearer interpretation of the data. Very constructive comments made by the reviewers (M. Bizimis, I. Savov and an anonymous reviewer) and the editors J. Ryan and V. Salters helped improve the content and clarity of the discussion.

References

Albarède, F., Simonetti, A., Vervoort, J.D., Blichert-Toft, J. and Abouchami, W., 1998. A Hf-Nd isotopic correlation in ferromanganese nodules. Geophysical Research Letters, 25(20): 3895-3898.

Alt, J.C., 2003. Stable isotopic composition of upper oceanic crust formed at a fast spreading ridge, ODP Site 801. Geochemistry Geophysics Geosystems, 4(5): 8908, doi:10.1029/2002GC000400.

Alt, J.C., France-Lanord, C., Floyd, P.A., Castillo, P.R. and Galy, A., 1992. Low-temperature hydrothermal alteration of jurassic ocean crust, Site 801. In: R.L. Larson, Y. Lancelot and e. al. (Editors), Proceedings of the Ocean Drilling Program, Scientific Results. Ocean Drilling Program, College Station, Tex., pp. 415-427.

Armstrong, R.L., 1968. A model for the evolution of strontium and lead isotopes in a dynamic Earth. Review of Geophysics, 6: 175-199.

Armstrong, R.L., 1991. The persistent myth of crustal growth. Australian Journal of Earth Sciences, 38: 613-630.

Barr, S.R., Révillon, S., Brewer, T.S., Harvey, P.K. and Tarney, J., 2002. Determining the inputs to the Mariana Subduction Factory: Using core-log integration to reconstruct basement lithology at ODP Hole 801C. Geochemistry Geophysics Geosystems, 3(11): 8901, doi:10.1029/2001GC000255.

Bartolini, A., 2003. Cretaceous radiolarian biochronology and carbon isotope stratigraphy of ODP Site 1149 (northwestern Pacific, Nadezhda Basin). Proceedings of the Ocean Drilling Program Scientific Results, 185: 17.

Bartolini, A. and Larson, R.L., 2001. Pacific microplate and the Pangea supercontinent in the Early to Middle Jurassic. Geology, 29(8): 735-738.

BenOthman, D., White, W.M. and Patchett, P.J., 1989. The geochemistry of marine sediments, island arc magma genesis, and crust-mantle recycling. Earth and Planetary Science Letters, 94: 1-21.

Bizimis, M., Salters, V.M. and Dawson, J.B., 2003. The brevity of carbonatite sources in the mantle: evidence from Hf isotopes. Contributions to Mineralogy and Petrology, 145(3): 281-300.

Blichert-Toft, J., 2001. On the Lu-Hf isotope geochemistry of silicate rocks. Geostandards Newsletter, 25(1): 41-56.

Blichert-Toft, J. and Albarède, F., 1997. The Lu-Hf isotope geochemistry of chondrites and the evolution of the mantle-crust system. Earth and Planetary Science Letters, 148: 243-258.

Blichert-Toft, J. and Albarède, F., 1999. Hf isotopic compositions of the Hawaii Scientific Drilling Project core and the source mineralogy of Hawaiian basalts. Geophysical Research Letters, 26(7): 935-938.

Blichert-Toft, J., Chauvel, C. and Albarède, F., 1997. Separation of Hf and Lu for high-precision isotope analysis of rock samples by magnetic sector-multiple collector ICP-MS. Contributions to Mineralogy and Petrology, 127: 248-260.

Castillo, P.R., Floyd, P.A. and France-Lanord, C., 1992. Isotope geochemistry of Leg 129 basalts: Implications for the origin of the widespread cretaceous volcanic event in the Pacific. In: R.L. Larson, Y. Lancelot and e. al. (Editors), Proceedings of the Ocean Drilling Program, Scientific Results. Ocean Drilling Program, College Station, Tex., pp. 405-413.

Chauvel, C. and Blichert-Toft, J., 2001. A hafnium isotope and trace element perspective on melting of the depleted mantle. Earth and Planetary Science Letters, 190: 137-151.

684 Chauvel, C., Hofmann, A.W. and Vidal, P., 1992. HIMU-EM: The French Polynesian
685 connection. Earth and Planetary Science Letters, 110: 99-119.
686 Chauvel, C., Lewin, E., Carpentier, M., Arndt, N.T. and Marini, J.-C., 2008. Role of
687 recycled oceanic basalt and sediment in generating the Hf-Nd mantle array.
688 Nature Geoscience, 1(1): 64-67.
689 Chauvel, C., McDonough, W., Guille, G., Maury, R. and Duncan, R., 1997.
690 Contrasting old and young volcanism in Rurutu Island, Austral Chain.
691 Chemical Geology, 139: 125-143.
692 Coffin, M.F., Lawver, L.A., Cahagan, L.M. and Campbell, D.A., 2000. The Plates
693 Project 2000 atlas of plate reconstructions (750 Ma to present day), University
694 of Texas, Plates Project Progress Report 250, Austin.
695 David, K., Frank, M., O'Nions, R.K., Belshaw, N.S. and Arden, J.W., 2001. The Hf
696 isotope composition of global seawater and the evolution of Hf isotopes in the
697 deep Pacific Ocean from Fe-Mn crusts. Chemical Geology, 178: 23-42.
698 Dimalanta, C., Taira, A., Jr., G.P.Y., Tokuyama, H. and Mochizuki, K., 2002. New
699 rates of western Pacific island arc magmatism from seismic and gravity data.
700 Earth and Planetary Science Letters, 202: 105-115.
701 Elliott, T., Plank, T., Zindler, A., White, W.M. and Bourdon, B., 1997. Element
702 transport from slab to volcanic front at the Mariana arc. Journal of
703 Geophysical Research, 102(B7): 14991-15019.
704 Fisk, M. and Kelley, K.A., 2002. Probing the Pacific's oldest MORB glass: mantle
705 chemistry and melting conditions during the birth of the Pacific Plate. Earth
706 and Planetary Science Letters, 202: 741-752.
707 Floyd, P.A. and Castillo, P.R., 1992. Geochemistry and petrogenesis of jurassic ocean
708 crust basalts, Site 801. In: R.L. Larson, Y. Lancelot and e. al. (Editors),
709 Proceedings of the Ocean Drilling Program, Scientific Results. Ocean Drilling
710 Program, College Station, Tex., pp. 361-388.
711 Floyd, P.A., Winchester, J.A. and Castillo, P.R., 1992. Geochemistry and petrography
712 of cretaceous sills and lava flows, Sites 800 and 802. In: R.L. Larson, Y.
713 Lancelot and e. al. (Editors), Proceedings of the Ocean Drilling Program,
714 Scientific Results. Ocean Drilling Program, College Station, Tex., pp. 345-
715 359.
716 Fryer, P., Taylor, B., Langmuir, C.H. and Hochstaedter, A.G., 1990. Petrology and
717 geochemistry of lavas from the Sumisu and Torishima backarc rifts. Earth and
718 Planetary Science Letters, 100: 161-178.
719 Georoc, April 2008. http://georoc.mpch-mainz.gwdg.de/georoc/.
720 Godfrey, L.V., Lee, D.-C., Sangrey, W.F., Halliday, A.N., Salters, V.J.M., Hein, J.R.
721 and White, W.M., 1997. The Hf isotopic composition of ferromanganese
722 nodules and crusts and hydrothermal manganese deposits: Implications for
723 seawater Hf. Earth and Planetary Science Letters, 151: 91-105.
724 Hauff, F., Hoernle, K. and Schmidt, A., 2003. Sr-Nd-Pb composition of Mesozoic
725 Pacific oceanic crust (Site 1149 and 801, ODP Leg 185): Implications for
726 alteration of ocean crust and the input into the Izu-Bonin-Mariana subduction
727 system. Geochemistry Geophysics Geosystems, 4(8): 8913,
728 doi:10.1029/2002GC000421.
729 Hickey-Vargas, R., 1998. Origin of the Indian Ocean-type isotopic signature in
730 basalts from Philippine Sea plate spreading centers: An assessment of local
731 versus large-scale processes. Journal of Geophysical Research, 103(B9):
732 20963-20979.
733 Hochstaedter, A.G., Gill, J.B., Kusakabe, M., Newman, S., Pringle, M.S., Taylor, B.
734 and Fryer, P., 1990a. Volcanism in the Sumisu Rift, I. Major element, volatile,

735 and stable isotope geochemistry. Earth and Planetary Science Letters, 100:
736 179-194.
737 Hochstaedter, A.G., Gill, J.B. and Morris, J.D., 1990b. Volcanism in the Sumisu Rift,
738 II. Subduction and non-subduction related components. Earth and Planetary
739 Science Letters, 100: 195-209.
740 Hochstaedter, A.G., Gill, J.B., Peters, R., Broughton, P., Holden, P. and Taylor, B.,
741 2001. Across-arc geochemical trends in the Izu-Bonin arc: Contributions from
742 the subducting slab. Geochemistry Geophysics Geosystems, 2: Paper number
743 2000GC000105.
744 Hochstaedter, A.G., Gill, J.B., Taylor, B., Ishizuka, O., Yuasa, M. and Morita, S.,
745 2000. Across-arc geochemical trends in the Izu-Bonin arc: Constraints on
746 source composition and mantle melting. Journal of Geophysical Research,
747 105(B1): 495-512.
748 Hofmann, A.W., 1988. Chemical differentiation of the Earth: The relationship
749 between mantle, continental crust, and oceanic crust. Earth and Planetary
750 Science Letters, 90: 297-314.
751 Hofmann, A.W. and White, W.M., 1982. Mantle plumes from ancient oceanic crust.
752 Earth and Planetary Science Letters, 57: 421-436.
753 Hussong, D.M., Uyeda, S. and al., e., 1982. Site 452: Mesozoic Pacific Ocean basin.
754 Initial Reports of the Deep Sea Drilling Project, 60: 77-93.
755 Ikeda, Y. and Yuasa, M., 1989. Volcanism in nascent back-arc basins behind the
756 Shichito Ridge and adjacent areas in the Izu-Ogasawara arc, northwest Pacific:
757 Evidence for mixing between E-type MORB and island arc magmas at the
758 initiation of back-arc rifting. Contributions to Mineralogy and Petrology, 101:
759 377-393.
760 Ishikawa, T. and Tera, F., 1999. Two isotopically distinct fluid components involved
761 in the Mariana arc: Evidence from Nb/B ratios and B, Sr, Nd, and Pb isotope
762 systematics. Geology, 27(1): 83-86.
763 Johnson, M.C. and Plank, T., 1999. Dehydration and melting experiments constrain
764 the fate of subducted sediments. Geochemistry, Geophysics, Geosystems, 1:
765 Paper number 1999GC000014.
766 Kelley, K.A., Plank, T., Ludden, J. and Staudigel, H., 2003. Composition of altered
767 oceanic crust at ODP Sites 801 and 1149. Geochemistry Geophysics
768 Geosystems, 4(6): 8910, doi:10.1029/2002GC000435.
769 Klimm, K., Blundy, J.D. and Green, T.H., 2008. Trace Element Partitioning and
770 Accessory Phase Saturation during H2O-Saturated Melting of Basalt with
771 Implications for Subduction Zone Chemical Fluxes. J. Petrology, 49(3): 523-
772 553.
773 Kogiso, T., Tatsumi, Y. and Nakano, S., 1997. Trace element transport during
774 dehydration processes in the subducted oceanic crust: 1. Experiments and
775 implications for the origin of ocean island basalts. Earth and Planetary Science
776 Letters, 148: 193-205.
777 Koppers, A.A.P., Staudigel, H. and Duncan, R.A., 2003a. High-resolution $^{40}Ar/^{39}Ar$
778 dating of the oldest oceanic basement basalts in the western Pacific basin.
779 Geochemistry Geophysics Geosystems, 4(11): 8914,
780 doi:10.1029/2003GC000574.
781 Koppers, A.A.P., Staudigel, H., Pringle, M.S. and Wijbrans, J.R., 2003b. Short-lived
782 and discontinuous intraplate volcanism in the South Pacific: Hot spots or
783 extensional volcanism? Geochemistry Geophysics Geosystems, 4(10).
784 Lancelot, Y., Larson, R.L. and al., e., 1990. Proceedings of the Ocean Drilling
785 Program, Initial Reports, 129. Ocean Drilling Program, College Station, Tex.,
786 488 p. pp.

787 Langmuir, C.H., Vocke, R.D., Hanson, G.N. and Hart, S.R., 1978. A general mixing
788 equation with applications to icelandic basalts. Earth and Planetary Science
789 Letters, 37: 380-392.
790 Lassiter, J.C., Blichert-toft, J., Hauri, E.H. and Barczus, H.G., 2004. Isotope and trace
791 element variations in lavas from Raivavae and Rapa, Cook-Austral Islands:
792 constraints on the nature of Himu-and EM-mantle and the origin of mid-plate
793 volcanism in French Polynesia. Chemical Geology, 202: 115-138.
794 Lees, G.J., Rowbotham, G. and Floyd, P.A., 1992. Petrography and Geochemistry of
795 graded volcaniclastic sediments and their clasts, Leg 129. In: R.L. Larson, Y.
796 Lancelot and e. al. (Editors), Proceedings of the Ocean Drilling Program,
797 Scientific Results. Ocean Drilling Program, College Station, Tex., pp. 137-
798 152.
799 LeFèvre, B. and Pin, C., 2001. An extraction chromatography method for Hf
800 separation prior to isotopic analysis using multiple collection ICP-Mass
801 spectrometry. Analytical Chemistry, 73(11): 2453-2460.
802 Ludden, J.N., Plank, T., Larson, R. and Escutia, C., 2006. Leg 185 Synthesis:
803 sampling the oldest crust in the ocean basins to understand Earth's geodynamic
804 and geochemical fluxes. In: J.N. Ludden, T. Plank and C. Escutia (Editors),
805 Proc. ODP Sci. Results, pp. 1-35.
806 McLennan, S.M., Taylor, S.R., Culloch, M.T.M. and Maynard, J.B., 1990.
807 Geochemical and Nd-Sr isotopic composition of deep-sea turbidites: crustal
808 evolution and plate tectonic associations. Geochimica et Cosmochimica Acta,
809 54: 2015-2050.
810 Notsu, K., Isshiki, N. and Hirano, M., 1983. Comprehensive strontium isotope study
811 of Quarternary volcanic rocks from the Izu-Ogasawara arc. Geochemical
812 Journal, 17: 289-302.
813 Patchett, P.J. and Tatsumoto, M., 1980. A routine high-precision method for Lu-Hf
814 isotope geochemistry and chronology. Contributions to Mineralogy and
815 Petrology, 75: 263-267.
816 Pearce, J.A., Kempton, P.D., Nowell, G.M. and Noble, S.R., 1999. Hf-Nd element
817 and isotope perspective on the nature and provenance of mantle and
818 subduction components in Western Pacific arc-basin systems. Journal of
819 Petrology, 40(11): 1579-1611.
820 PetDB, April 2008. http://www.petdb.org.
821 Pfänder, J.A., Münker, C., Stracke, A. and Mezger, K., 2007. Nb/Ta and Zr/Hf in
822 ocean island basalts - Implications for crust-mantle differentiation and the fate
823 of Niobium. Earth and Planetary Science Letters, 254: 158-172.
824 Piepgras, D.J. and Jacobsen, S.B., 1988. The isotopic composition of neodymium in
825 the North Pacific. Geochimica et Cosmochimica Acta, 52: 1373-1381.
826 Plank, T., Kelley, K.A., Murray, R.W. and Stern, L.Q., 2007. Chemical composition
827 of sediments subductiong at the Izu-Bonin trench. Geochemistry Geophysics
828 Geosystems, 8(4): Q04I16.
829 Plank, T. and Langmuir, C.H., 1998. The chemical composition of subducting
830 sediment and its consequences for the crust and mantle. Chemical Geology,
831 145: 325-394.
832 Plank, T., Ludden, J.N., Escutia, C. and al., e., 2000. Proceedings of the Ocean
833 Drilling Program, Initial Reports, 185. Ocean Drilling Program, College
834 Station, Tex.
835 Plank, T. and van Keken, P.E., 2008. The ups and downs of sediments. Nature
836 Geoscience, 1(1): 17-18.
837 Pringle, M.S., 1992. Radiometric ages of basaltic basement recovered at Sites 800,
838 801, and 802, Leg 129, Western Pacific Ocean. In: R.L. Larson, Y. Lancelot

and e. al. (Editors), Proceedings of the Ocean Drilling Program, Scientific Results. Ocean Drilling Program, College Station, Tex., pp. 389-404.
Reisberg, L., Rouxel, O., Ludden, J., Staudigel, H. and Zimmermann, C., 2008. Re-Os results form ODP Site 801: Evidence for extensive Re uptake during alteration of oceanic crust. Chemical Geology, 248: 256-271.
Revillon, S., 2000. Origine et composition du Plateau Océanique Caraïbe. Mémoires Géosciences Rennes, 97, 358 pp.
Ryan, J.G. and Langmuir, C.H., 1988. Beryllium systematics in young volcanic rocks: Implications for 10Be. Geochimica et Cosmochimica Acta, 52(1): 237-244.
Salters, V.J.M. and Stracke, A., 2004. Composition of the depleted mantle. Geochemistry Geophysics Geosystems, 5: Q05004.
Savov, I.P., Hickey-Vargas, R., D'Antonio, M., Ryan, J.G. and Spadea, P., 2006. Petrology and Geochemistry of West Philippine Basin Basalts and Early Palau-Kyushu Arc Volcanic Clasts from ODP Leg 195, Site 1201D: Implications for the Early History of the Izu-Bonin-Mariana Arc. J. Petrology, 47(2): 277-299.
Schmidt, A., 2001. Temporal and spatial evolution of the Izu island arc, Japan, in terms of Sr-Nd-Pb isotope geochemistry, University of Kiel, Kiel, 81 pp.
Shimizu, H., Tachikawa, K., Masuda, A. and Nozaki, Y., 1994. Cerium and neodymium isotope ratios and REE patterns in seawater from the North Pacific Ocean. Geochimica et Cosmochimica Acta, 58: 323-333.
Staudigel, H., Davies, G.R., Hart, S.R., Marchant, K.M. and Smith, B.M., 1995. Large scale isotopic Sr, Nd and O isotopic anatomy of altered oceanic crust: DSDP/ODP sites 417/418. Earth and Planetary Science letters, 130: 169-185.
Staudigel, H., Park, K.-H., Pringle, M.S., Rubenstone, J.L., Smith, W.H.F. and Zindler, A., 1991. The longevity of the South Pacific isotopic and thermal anomaly. Earth and Planetary Science Letters, 102: 24-44.
Stern, R., Kohut, E., Bloomer, S., Leybourne, M., Fouch, M. and Vervoort, J., 2006. Subduction factory processes beneath the Guguan cross-chain, Mariana Arc: no role for sediments, are serpentinites important? Contributions to Mineralogy and Petrology, 151(2): 202-221.
Straub, S.M., 2003. The evolution of the Izu Bomin - Mariana volcanic arcs (NW Pacific) in terms of major element chemistry. Geochemistry Geophysics Geosystems, 4(2): 33.
Straub, S.M. and Layne, G.D., 2002. The systematics of boron isotopes in Izu arc front volcanic rocks. Earth and Planetary Science Letters, 198: 25-39.
Straub, S.M., Layne, G.D., Schmidt, A. and Langmuir, C.H., 2004. Volcanic glasses at the Izu arc volcanic front: New perspectives on fluid and sediment melt recycling in subduction zones. Geochemistry Geophysics Geosystems, 5(1): 40.
Talbi, E.H. and Honnorez, J., 2003. Low-temperature alteration of mesozoic oceanic crust, Ocean Drilling Program Leg 185. Geochemistry Geophysics Geosystems, 4(5): 8906, doi:10.1029/2002GC000405.
Tatsumi, Y., Murasaki, M. and Nohda, S., 1992. Across-arc variation of lava chemistry in the Izu-Bonin arc: Identification of subduction components. Journal of Volcanology and Geothermal Research, 49: 179-190.
Taylor, R.N. and Nesbitt, R.W., 1998. Isotopic characteristics of subduction fluids in an intra-oceanic setting, Izu-Bonin arc, Japan. Earth and Planetary Science Letters, 164: 79-98.
Tera, F., Brown, L., Morris, J., Sacks, I.S., Klein, J. and Middleton, R., 1986. Sediment incorporation in island-arc magmas: Inferences from 10Be. Geochimica et Cosmochimica Acta, 50(4): 535-550.

Tollstrup, D.L. and Gill, J.B., 2005. Hafnium systematics of the Mariana arc: Evidence for sediment melt and residual phases. Geology, 33(9): 731-740.

van de Flierdt, T., Goldstein, S.L., Hemming, S.R., Roy, M., Frank, M. and Halliday, A.N., 2007. Global neodymium-hafnium isotope systematics -- revisited. Earth and Planetary Science Letters, 259(3-4): 432.

Vervoort, J.D., Patchett, P.J., Blichert-Toft, J. and Albarède, F., 1999. Relationships between Lu-Hf and Sm-Nd isotopic systems in the global sedimentary system. Earth and Planetary Science Letters, 168: 79-99.

Vlastelic, I., Carpentier, M. and Lewin, E., 2005. Miocene climate change recorded in the chemical and isotopic (Pb, Nd, Hf) signature of Southern Ocean sediments. Geochemistry, Geophysics, Geosystems, 6: Q03003.

VonHuene, R. and Scholl, D.W., 1991. Observations at convergent margins concerning sediment subduction, subduction erosion, and the growth of continental crust. Review of Geophysics, 29: 279-316.

VonHuene, R. and Scholl, D.W., 1993. The return of sialic material to the mantle indicated by terrigenous material subducted at convergent margins. Tectonophysics, 219: 163-175.

Wade, J.A., Plank, T., Stern, R.J., Tollstrup, D.L., Gill, J.B., O'Leary, J.C., Eiler, J.M., Moore, R.B., Woodhead, J.D., Trusdell, F., Fischer, T.P. and Hilton, D.R., 2005. The May 2003 eruption of Anatahan volcano, Mariana Islands: Geochemical evolution of a silicic island-arc volcano. Journal of Volcanology and Geothermal Research, 146: 139-170.

White, W.M. and Patchett, P.J., 1984. Hf-Nd-Sr isotopes and incompatible element abundances in island arcs: implications for magma origins and crust-mantle evolution. Earth and Planetary Science Letters, 67: 167-185.

White, W.M., Patchett, P.J. and Othman, D.B., 1986. Hf isotope ratios of marine sediments and Mn nodules: evidence for a mantle source of Hf in seawater. Earth and Planetary Science Letters, 79: 46-54.

Woodhead, J.D., 1989. Geochemistry of the Mariana arc (western Pacific): Source composition and processes. Chemical Geology, 76: 1-24.

Woodhead, J.D., Hergt, J.M., Davidson, J.P. and Eggins, S.M., 2001. Hafnium isotope evidence for 'conservative' element mobility during subduction zone processes. Earth and Planetary Science Letters, 192: 331-346.

Figures captions

Figure 1 Map of the Western Pacific region with locations of ODP Sites 800, 801, 802, 1149 and DSDP Site 452 (modified from Plank et al. (2000)).

Figure 2 Lithostratigraphic column of Site 1149 with locations of samples analyzed for Hf and Nd isotopes. The transition between subunit IIB and unit III consists of zeolitic clays extremely enriched in REE relative to other Site 1149 sediments (Plank et al., 2007). They have been considered as a distinct unit in this study.

Figure 3 ε_{Hf} vs. ε_{Nd} diagram showing the measured and initial isotopic compositions of the composite basalts from Hole 801C relative to measurements published by Pearce et al. (1999) and the fields of present-day MORB and OIB. For the MORB composites, ε_{Nd} and ε_{Hf}, and $\varepsilon_{Nd(i)}$ and $\varepsilon_{Hf(i)}$ are almost identical and are shown by only one symbol. In contrast, a difference of one to two ε values is observed for the alkali basalts and the measured values are shown by the light color symbols while the initial values are shown by the orange dots. The HIMU islands in the Austral chain (Tubuai, Rurutu and Raevavae) are shown with darker symbols. The inset in the upper left corner presents the initial ε_{Hf} and ε_{Nd} with uncertainties of about ±0.65 unit for the $\varepsilon_{Nd(i)}$ values and about ±1 unit for the $\varepsilon_{Hf(i)}$ values. MORB and OIB data are compiled from Georoc and PetDB databases (Georoc; PetDB) as well as unpublished data from C. Chauvel.

Figure 4 $\varepsilon_{Nd(i)}$ and $\varepsilon_{Hf(i)}$ values of Site 1149 sediments plotted versus depth in the sedimentary pile.

Figure 5 $\varepsilon_{Hf(i)}$ vs. $\varepsilon_{Nd(i)}$ diagram comparing the initial ratios calculated for Site 1149 sediments with those of Fe-Mn crusts and nodules and other oceanic sediments. Samples 7H4 140-150, 10H3 140-150, 16R1 93-98 and 29R1 28-35, with distinct features are marked. The Nd isotopic composition of sample 29R1 is from Hauff et al. (2003). Fe-Mn crusts and nodules and other sediments data are from White et al. (1986), Ben Othman et al. (1989), McLennan et al. (1990), Godfrey et al. (1997), Albarède et al. (1998), Pearce et al. (1999), Vervoort et al. (1999) and David et al. (2001). "Terrestrial array" as defined by Vervoort et al. (1999) is also shown. MORB data sources as in Figure 3.

Figure 6 Sm/Nd vs. $\varepsilon_{Nd(i)}$ diagram showing Site 1149 sediments together with the Pacific Seawater field, the Izu-Mariana arc lavas, the Site 800A alkali dolerites and OIB from Magellan seamounts. Trace element data of Site 1149 sediments are from Plank et al. (2007). The Pacific Seawater field has been drawn using data published by Piepgras et al. (1988) and Shimizu et al. (1994). Izu-Mariana arc lavas are from White et al. (1984), Woodhead et al. (1989), Elliott et al. (1997), Pearce et al. (1999), Woodhead et al. (2001), Wade et al. (2005), Tollstrup and Gill (2005) and Stern et al. (2006). Four sediments analyzed by Pearce et al. (1999) are shown with small brown dots. Site 800A dolerites data are from Floyd et al. (1992) and Castillo et al. (1992). Magellan seamounts data are from Staudigel et al. (1991).

Figure 7 Present-day ε_{Hf} vs. ε_{Nd} diagram of Site 1149 sediments together with Fe-Mn crusts and nodules and other oceanic sediments. Hf and Nd isotopes of a composite from DSDP Site 452 sedimentary pile are from Woodhead et al. (1989) while values for Site 801 are from Wade et al. (2005). Other data sources as in Figure 5. The positions of Site 1149 sediments in the figure differ slightly from their position in

977 Figure 5 because here we plot present-day measured ratios while initial ratios were
978 reported in Figure 5.
979
980 **Figure 8** $^{176}Hf/^{177}Hf$ vs. $^{143}Nd/^{144}Nd$ for sediments, Izu-Bonin-Mariana arc lavas and
981 Pacific and Indian MORB showing that less than 2% sediment combined with Pacific
982 MORB mantle is enough to explain the composition of the arc lavas. The sediment
983 composition of Site 1149 is given in Table 4 and the depleted mantle compositions
984 are evaluated as follows: (a) Nd and Hf concentrations are from Salters and Stracke
985 (2004); (b) three different isotopic compositions were selected: our estimated average
986 composition for Pacific MORB: ε_{Nd}=+9.7 and ε_{Hf}=+15, the sample with the most
987 radiogenic Hf isotopes: ε_{Nd}=+10.8 and ε_{Hf}=+20.1, and the sample with the least
988 radiogenic Hf isotopes: ε_{Nd}=+11.2 and ε_{Hf}=+12.1. Three mixing arrays are shown
989 between sediment and the three depleted mantle sources. The mixing arrays were
990 calculated assuming bulk mixtures of sediment and mantle. The sediment proportions
991 are therefore maximum proportions because if the sediment component is extracted
992 through either a melt or a fluid phase, the trace element concentrations of the
993 contaminant should be higher than the starting sediment concentrations. The mixing
994 array between Site 801 estimate (Wade et al., 2005) and average Pacific mantle
995 shown with a dashed brown curve passes well below the arc lava fields. If an Indian-
996 type mantle is used instead of a Pacific depleted mantle, the proportion of sediment
997 required to explain the Izu-Mariana arc data is even lower, at less than 1%. Data
998 sources as in figures 4, 5 and 6 plus sediment data from Vlastelic et al. (2005) and
999 Philippine plate basement and volcanic clasts from Pearce et al. (1999) and Savov et
1000 al. (2006).
1001

Figure 9 (a) Hf/Hf* vs. ε_{Hf} and (b) Nd/Hf vs. ε_{Hf} showing mixing arrays between the average Site 1149 sediment and the same three potential depleted mantle sources as in Figure 8. With the exception of the Kasuga seamounts and the Izu protoarc volcanics, most Izu and Mariana arc volcanics can be explained by less than 4% sediment in the contaminated mantle source. Calculations were performed as in Figure 8 and the data sources are as in figures 5,6,7 and 8. Hf/Hf* measures the size of the primitive mantle normalized Hf anomaly calculated using the following equation: $Hf/Hf^*=Hf_N/((Nd_N+Sm_N)/2)$ and the normalizing values of Hofmann (1988) . As in Figure 8, the mixing array between Site 801 estimate (Wade et al., 2005) and depleted mantle does not intersect the island arc data field.

Figure 10 ε_{Hf} versus ε_{Nd} diagram showing the relationship between island arc volcanics and oceanic sediments. The island arc array is shown by an orange line while the mantle array is shown by a grey line. Field for the three main types of oceanic sediments are from Chauvel et al. (2008) and data on circum-Antarctic sediments published by van de Flierdt et al. (2007) are also shown (light brown diamants) but could not be distributed among the fields due to the absence of petrological description. Because no ε_{Hf} value is available for GLOSS, its composition is represented by a vertical brown bar at ε_{Nd} = -8.9. Two typical mixing arrays calculated using the GLOSS Nd and Hf concentrations and mantle values as given in the caption of Figure 8 are shown as brown thin curves: one using an elevated ε_{Hf} value at about + 4 and one using a low ε_{Hf} value at -13. A mixing curve between Site 1149 and depleted mantle is also shown (black dashed curve). Data were compiled using the Georoc database (Georoc, April 2008) for IAV and OIB and the PetDB database (PetDB, April 2008) for MORB.

Table 1: Hf and Nd isotopic compositions of Hole 801C Composites

Composites[a]	Type	$^{143}Nd/^{144}Nd \pm 2\sigma_m$[b]	ε_{Nd}[c]	$\varepsilon_{Nd}(i)$[d]	$^{176}Hf/^{177}Hf \pm 2\sigma_m$[b]	ε_{Hf}[c]	$\varepsilon_{Hf}(i)$[d]
801-TAB-0-50	FLO	0.512845 ± 13	+4.0	+5.4	0.282979 ± 7	+7.3	+9.9
801-TAB-0-50	VCL	0.512848 ± 9	+4.1	+5.4	0.283019 ± 6	+8.7	+10.9
801-TAB-0-50	All	0.512896 ± 6	+5.0	+6.3	0.282973 ± 5	+7.1	+9.6
801-MORB-0-110	FLO	0.513154 ± 32	+10.1	+9.7	0.283206 ± 6	+15.3	+15.8
801-MORB-0-110	All	0.513081 ± 10	+8.6	+8.3	0.283201 ± 5	+15.2	+15.3
801-MORB-110-220	FLO	0.513128 ± 9	+9.6	+9.2	0.283171 ± 6	+14.1	+14.8
801-MORB-110-220	VCL	0.513080 ± 6	+8.6	+8.4	0.283219 ± 9	+15.8	+15.4
801-MORB-110-220	All	0.513103 ± 7	+9.1	+8.8	0.283194 ± 8	+14.9	+15.4
801-MORB-220-420	FLO	0.513154 ± 8	+10.1	+9.8	0.283172 ± 7	+14.1	+14.7
801-MORB-220-420	VCL	0.513157 ± 5	+10.1	+9.8	0.283201 ± 5	+15.2	+15.7
801-MORB-220-420	VCL[e]	0.513159 ± 4	+10.2	+9.9			
801-MORB-220-420	All	0.513132 ± 7	+9.6	+9.3	0.283161 ± 6	+13.8	+14.3
801	SUPER	0.513118 ± 6	+9.4	+9.1	0.283164 ± 7	+13.9	+14.3

Footnote:

[a] TAB, top alkali basalts; MORB, mid-ocean ridge tholeiites; FLO, less altered flows and pillows; VCL, highly altered volcanoclastics; SUPER, all site 801 tholeiite.

[b] Normalized for mass fractionation to $^{146}Nd/^{144}Nd=0.7219$ and $^{179}Hf/^{177}Hf=0.7325$.

[c] εHf and ε_{Nd} have been calculated using $^{176}Hf/^{177}Hf_{CHUR}=0.282772$ after Blichert-Toft and Albarède, 1997 and $^{143}Nd/^{144}Nd_{CHUR}=0.512638$.

[d] εHf(i) and $\varepsilon_{Nd}(i)$ have been calculated using the trace element data published by Kelley et al. (2003) and the following ages: alkali materials 157Ma and tholeiitic materials 167Ma (Pringle, 1992); $^{176}Lu/^{177}Hf_{CHUR(0)}=0.0332$ after Blichert-Toft and Albarède, 1997 and $^{147}Sm/^{144}Nd_{CHUR(0)}=0.1967$.

[e] Complete duplicate analysis.

Table 2: Hf and Nd isotopic compositions of Site 1149 sediments

Sample	Depth (mbsf)[a]	Unit	Dissolution	Protocol[b]	$^{143}Nd/^{144}Nd \pm 2\sigma_m$[c]	ε_{Nd}[d]	$\varepsilon_{Nd(i)}$[e]	$^{176}Hf/^{177}Hf \pm 2\sigma_m$[c]	ε_{Hf}[d]	$\varepsilon_{Hf(i)}$[e]
1149A 1H1 140-150	1.40	I		BT 97	0.512369 ± 10	-5.2	-5.2	0.282966 ± 8	+6.9	+6.9
1149A 1H1 140-150[f]	1.40	I	in Parr Bomb	BT 97				0.282964 ± 5[g]	+6.8	+6.8
1149A 4H2 140-150	26.10	I		BT 97	0.512307 ± 5	-6.5	-6.4	0.282939 ± 9	+5.9	+5.9
1149A 4H2 140-150[f]	26.10	I		BT 97	0.512271 ± 6	-7.2	-7.2			
1149A 7H4 140-150	57.60	I		BT 97	0.512557 ± 6	-1.6	-1.6	0.283063 ± 8	+10.3	+10.3
1149A 10H3 140-150	84.60	I		BT 97	0.512483 ± 4	-3.0	-3.0	0.282973 ± 4[g]	+7.1	+7.1
1149A 10H3 140-150[f]	84.60	I		BT 97	0.512507 ± 5	-2.6	-2.5			
1149A 14H2 140-150	121.10	IIA		BT 97	0.512291 ± 11	-6.8	-6.6	0.282960 ± 6[g]	+6.6	+6.7
1149A 18H3 140-150	160.40	IIB	in Parr Bomb	BT 97				0.282816 ± 8	+1.6	+1.6
1149A 18H3 140-150[f]	160.40	IIB	in Parr Bomb	BT 97				0.282791 ± 4	+0.7	+0.7
1149A 20X1 140-150	171.20	IIB-III		BT 97	0.512342 ± 5	-5.8	-5.4	0.282936 ± 5[g]	+5.8	+3.7
1149B 6R1 38-42	199.08	III	in Parr Bomb	Ca-Depl	0.512308 ± 6	-6.4	-5.8	0.282873 ± 8[g]	+3.6	+2.2
1149B 12RCC 0-5	245.40	III	in Parr Bomb	Ca-Depl	0.512294 ± 5	-6.7	-5.8	0.282761 ± 3	-0.4	-1.4
1149B 16R1 93-98	283.23	IV		BT 97	0.512519 ± 6	-2.3	-1.1	0.282954 ± 6	+6.4	+8.0
1149B 17R1 14-17	292.14	IV		BT 97	0.512248 ± 12	-7.6	-6.3	0.282677 ± 4	-3.4	-2.7
1149B 17R1 14-17[f]	292.14	IV		BT 97				0.282678 ± 3[g]	-3.3	-2.7
1149B 18R1 41-43	302.01	IV		BT 97	0.512269 ± 5	-7.2	-5.9	0.282692 ± 5	-2.8	-3.1
1149B 20R1 25-35	321.15	IV		BT 97	0.512267 ± 7	-7.2	-5.8			
1149B 22R1 20-25	340.30	IV		BT 97	0.512240 ± 8	-7.8	-6.5	0.282671 ± 23	-3.6	-3.3
1149B 25R1 19-23	368.89	IV	in Parr Bomb	Ca-Rich				0.282715 ± 9[g]	-2.0	-5.4
1149B 27R1 49-55	388.09	IV		Ca-Rich	0.512282 ± 12	-6.9	-5.5			
1149B 28R1 52-56	397.62	IV		BT 97	0.512353 ± 77	-5.6	-4.1			
1149B 28R2 48-66	398.90	IV		BT 97	0.512312 ± 24	-6.4	-4.9			
1149B 29R1 28-35	407.08	IV		BT 97				0.283244 ± 49	+16.7	+12.0

Footnote:

[a] mbsf, meters below surface seafloor.
[b] Protocol used for Hf separation: BT 97, original protocol of Blichert-Toft et al., 1997; Ca-Depl and Ca-Rich, protocols for Ca-depleted and Ca enriched samples described in Fig. A in the appendix.
[c] Normalized for mass fractionation to $^{146}Nd/^{144}Nd=0.7219$ and $^{179}Hf/^{177}Hf=0.7325$.
[d] ε_{Hf} and ε_{Nd} have been calculated using $^{176}Hf/^{177}Hf_{CHUR}=0.282772$ after Blichert-Toft and Albarède, 1997 and $^{143}Nd/^{144}Nd_{CHUR}=0.512638$.
[e] $\varepsilon_{Nd(i)}$ and $\varepsilon_{Hf(i)}$ have been calculated using the Sm/Nd and Lu/Hf ratios calculated from the trace element data published by Plank (2007) and for Unit I, III and IV sediments paleomagnetic and biostratigraphic ages reported by Plank et al., 2000. Approximate ages of samples from unit II were determined by linear extrapolation from ages of unit I and III samples using a constant sedimentation rate of 1 m/Ma, $^{176}Lu/^{177}Hf_{CHUR(0)}=0.0332$ after Blichert-Toft and Albarède, 1997 and $^{147}Sm/^{144}Nd_{CHUR(0)}=0.1967$. Assuming a 5% error on the measured parent/daughter ratios, the error propagation on the calculated $\varepsilon_{(i)}$ due to the trace element ratio is always smaller than 0.1 epsilon unit.
[f] Complete duplicate analysis.
[g] Data published by Chauvel et al. (2008).

Table 3: Hf and Nd bulk isotopic compositions and trace element ratios for the Site 1149 sedimentary pile

Unit	Mass%	$^{143}Nd/^{144}Nd$[a]	ε_{Nd}[b]	$^{176}Hf/^{177}Hf$[a]	ε_{Hf}[b]	Nd (ppm)[c]	Sm (ppm)[c]	Lu (ppm)[c]	Hf (ppm)[c]	Sm/Nd	Nd/Hf	Lu/Hf
Site 1149	100	0.512336	-5.9	0.282897	+4.4	25.2	5.32	0.39	1.44	0.211	17.5	0.271
Unit I	30.2	0.512423	-4.2	0.282987	+7.6	21.5	4.72	0.414	2.62	0.220	8.2	0.158
Subunit IIA	6.5	0.512291	-6.8	0.282960	+6.6	26.5	5.90	0.521	3.05	0.223	8.7	0.171
Subunit IIB	4.3			0.282816	+1.6	59.4	13.3	0.994	4.14	0.224	14.3	0.240
Subunit IIB-III	2.2	0.512342	-5.8	0.282936	+5.8	193.5	44.0	3.19	4.47	0.227	43.3	0.714
Unit III	24.4	0.512296	-6.7	0.282779	+0.2	30.5	6.34	0.531	1.38	0.208	22.1	0.385
Sample 16R1 93-98	0.04	0.512519	-2.3	0.282954	+6.4	37.9	7.44	0.541	5.24	0.196	7.2	0.103
Unit IV	32.2	0.512277	-7.0	0.282680	-3.3	11.5	2.17	0.142	0.48	0.189	24.0	0.296
Sample 29R1 28-35	0.2			0.283244	+16.7	20.1	3.74	0.332	0.55	0.186	36.5	0.604

Footnote:

[a] The isotopic composition of each unit has been calculated using the isotopic compositions and the Nd and Hf concentrations of discrete samples analyzed in each unit. The Nd and Hf isotopic compositions of the entire Site 1149 sedimentary pile have been calculated combining the isotopes, trace element compositions and mass % of each unit and the mixing equation of Langmuir et al. (1978). The trace element contents listed for the Site 1149 are from Plank et al. (2007).

[b] ε_{Hf} and ε_{Nd} have been calculated using $^{176}Hf/^{177}Hf_{CHUR}=0.282772$ after Blichert-Toft and Albarède, 1997 and $^{143}Nd/^{144}Nd_{CHUR}=0.512638$.

[c] Trace element data used for calculations. They differ slightly from values suggested by Plank et al. (2007) for individual units because we fell more comfortable calculating the average Nd and Hf isotopic compositions using samples that had been analyzed for isotopes instead of using the whole range of concentrations that vary quite widely in some of the units. The concentrations given on the first line for the entire Site 1149 are from Plank et al. (2007).

Table 4 Volcanic output and sediment input fluxes in the Izu subduction zone

	Output Flux	Sediment Flux	Mantle wedge
Volume ($x10^{-6}$ km^3/km/yr)	65.5 [a]	28.6 [c]	
Density (g/cm^3)	2.8	1.74 [d]	
wt% water		31.6 [d]	
Total dry flux ($x10^9$ kg/km/yr)	0.183	0.03399	
Average Nd conc. (ppm)	7.5 [b]	25.2 [d]	
ε_{Nd} value	+7 to +9 [e]	-5.9 [e]	+9.7 [f]
Nd flux (kg/km/yr)	1375	857	
Average Hf conc. (ppm)	1.7 [b]	1.44 [d]	
Hf flux (kg/km/yr)	312	49	
Nd/Hf	4.41	17.5	

Footnote:
[a] Average value for Izu-Bonin of Dimalanta et al. (2002).
[b] Average values of data from White & Patchett (1984) and Pearce et al. (1999).
[c] Calculated with a subduction rate of 7 cm/yr and a sediment thickness of 410 m.
[d] Data from Plank et al. (2007).
[e] Range of values of data from White & Patchett (1984) and Pearce et al. (1999) for the arc lavas.
[f] Average value of Pacific MORB.

Appendix:

Optimization of the chemical purification

The analytical procedure for Hf separation was based on the method published by Blichert-Toft et al. (1997) which proved to be highly efficient for most of the Site 801C composites and Site 1149 sediments, but failed for two particular sample groups and had to be modified: (1) The Hf isolation was unsuccessful for cherts and porcelanites collected at Site 1149. For these samples, Hf was not efficiently separated from heavy rare earth elements (HREE), and the Hf isotopic measurements on the P54 were disturbed by isobaric interferences at mass 176 caused by Yb and Lu. (2) The Hf chemical separation was poorly efficient for Ca-rich samples such as the marl and chalk but also for two basalt composites containing calcareous interpillow sediments. For these samples, the Hf recovery was extremely low and often insufficient for a proper isotopic measurement on the P54.

In the analytical procedure of Blichert-Toft et al. (1997) Hf is separated from the HREE using a HF leaching technique after sample dissolution. The REE precipitate into Ca-Mg fluoride salts while Hf remains in solution in the supernatant. For most samples, this procedure allows an almost complete recovery of Hf in the supernatant solution whereas virtually 100% of the REE are trapped into the Ca-Mg fluoride salts (Blichert-Toft et al., 1997). However, Blichert-Toft (2001) has shown that this procedure is inadequate to separate Hf from REE in Mg-rich samples (such as komatiites or picrites) because during the fluoride precipitation stage, Hf is entrained with the REE leading to low Hf recovery in the supernatant. Blichert-Toft (2001) suggested that the presence of high concentrations of Hf in the fluorides salts was probably due to high partition coefficients for Hf in Mg–rich fluorides.

1110 The low Hf recovery we experienced for Ca-rich samples suggests that a similar Hf
1111 precipitation occurs during HF leaching of Ca-rich materials. On the other hand, the
1112 very low Mg and Ca contents of cherts and porcelanites (CaO and MgO usually lower
1113 than 1%) could explain why HREE did not quantitatively precipitate into the fluoride
1114 salts during the HF leaching procedure. To confirm this interpretation, we performed
1115 experiments on the partitioning of Zr, Hf and REE during HF leaching and fluoride
1116 precipitation in Ca-rich and Ca-depleted samples. Three test samples were selected on
1117 the basis of their major elements (Table A): one basalt from the Sunda arc moderately
1118 enriched in CaO (CaO = 8.38%), one limestone from southeast France rich in CaO
1119 (CaO = 50.61%) and one andesite from the Sunda arc with a particularly low CaO
1120 (CaO = 0.7%). All three samples have low MgO (3.8%, 0.6% and 5.24% respectively)
1121 precluding potential trapping of HFSE in Mg-rich fluorides.
1122 Powders of the three samples were dissolved in savillex beakers with an HF:HNO_3
1123 mixture (≈ 6:1) at about 140°C for 48h and residues were leached 3 times with
1124 concentrated HF as recommended by Blichert-Toft et al. (1997). HF supernatant
1125 solutions and Ca-Mg fluoride salts were prepared for ICP-MS analysis with the
1126 exception of the fluorides formed by the Ca-rich sample because this residue resisted
1127 acid digestion and could not be put into solution. Percentages of REE, Zr and Hf
1128 recovered in each fraction are given in Table A and plotted in figures A 1&2. For the
1129 basalt moderately enriched in Ca, the measured REE, Hf and Zr partitioning between
1130 Ca-Mg fluoride salts and HF supernatant are similar to the results of Blichert-Toft et
1131 al. (1997). More than 97% of Zr and Hf are in the HF supernatant (figure A.1) while
1132 over 95% of the REE are in the fluoride precipitate. Among the REE, Ce is an
1133 exception with only 71% in the salt, probably because of the presence of both Ce^{3+}
1134 and Ce^{4+}. As mentioned above, the fluoride salts of the Ca-rich sample could not be
1135 analyzed but nevertheless only 2.2% of Zr and 0.9% of Hf were recovered in the HF

supernatant solution (Table A). This result demonstrates that during HF leaching of Ca-rich material, Zr and Hf are partitioned into the fluoride residue instead of staying in solution in HF. This suggests that Zr and Hf have significantly higher partition coefficients for Ca-rich fluorides than for Ca-poor fluorides. In contrast to the other two samples, the Ca-depleted andesite shows distinctive features (see Figure A.2): Zr and Hf are almost exclusively present in the HF supernatant (more than 99% of Zr and Hf) but the REE are also present in the leachate and show a progressive fractionation with the LREE mainly concentrated in the fluoride salt (over 80%) and the HREE distributed equally between the residue and the leachate (59% of Yb in the supernatant). Such distribution suggests a progressive decrease of the partition coefficient from LREE to HREE in the Ca-depleted fluoride salts and an inefficient separation of the REE from the HFSE using the HF leaching technique in such samples.

Our experiments demonstrate therefore that the Ca content plays a fundamental role on the distribution of HFSE and REE between fluoride salts and supernatant solution during HF leaching. For moderately Ca-rich matrices, HFSE are preferentially concentrated in the leachate while REE precipitate in the fluorides; for Ca-rich samples, HFSE and REE precipitate together in the fluoride residue; and finally for Ca-depleted samples, HFSE remain in the leachate while REE are evenly distributed between fluoride salts and HF supernatant solution. Despite providing excellent results for most rocks, the HF leaching procedure of Blichert-Toft et al. (1997) proves not to be efficient to separate Hf from REE in Ca-rich and Ca-poor samples and the original protocol of Blichert-Toft et al.(1997) has to be modified for this type of rock samples.

For Ca-rich samples, the HF leaching and fluoride precipitation step should be replaced by a cation-exchange column separation as published by Patchett (1980) and

1162 modified by Revillon et al. (Revillon, 2000). However this modified protocol
1163 succeeds only if Ca-rich fluorides salts do not precipitate during dissolution of the
1164 sample. These fluorides, very resistant to acid dissolution, are likely to contain large
1165 amounts of Hf leading to low Hf recovery. We suggest therefore that dissolution of
1166 Ca-rich samples should be achieved either using the procedure recommended by
1167 Bizimis et al. (2003)or using concentrated HF associated to large amounts of $HClO_4$
1168 or using lithium metaborate fusion as described in Lefèvre and Pin (2001). For Ca-
1169 depleted samples, the modified procedure consists simply in a column separation
1170 using cation-exchange resin instead of Hf leaching. In this case, REE are recovered
1171 from the cation-exchange column. In all cases, Nd is further isolated from the other
1172 REE using Eichrom® HDEHP-coated teflon resin.

1173
1174
1175

1176 **Appendix Figure A** REE, Zr and Hf distributions between supernatant and fluoride
1177 salts after HF leaching of (1) a sample moderately enriched in Ca and (2) a Ca-
1178 depleted sample.

1179

Appendix Table A: Trace element distributions after HF leaching of Ca-moderately enriched, Ca-highly enriched and Ca-depleted samples.

Sample	80J102[a]	287C[b]	PC6B[a]
Rock Type	Basalt	Limestone	Andesite
Location	Sunda arc	SE France	Sunda arc
CaO%	8.38	50.61	0.70
MgO%	3.80	0.60	5.24

Element [c]	Fluoride (%)	Supernatant (%)	Supernatant (%)	Fluoride (%)	Supernatant (%)
La	93.4	6.6	0	89.5	10.5
Ce	71.5	28.5	0	6.2	93.8
Pr	95.8	4.2	0	86.5	13.5
Nd	96.2	3.8	0	84.7	15.3
Sm	96.8	3.2	0	74.7	25.3
Zr	3.7	96.3	0.2	0.6	99.4
Hf	3.6	96.4	0	1.0	99.0
Eu	95.8	4.2	0.1	68.2	31.8
Gd	94.9	5.1	0	61.9	38.1
Tb	96.9	3.1	0	55.2	44.8
Dy	97.1	2.9	0	50.5	49.5
Ho	97.1	2.9	0	47.0	53.0
Er	97.1	2.9	0	43.7	56.3
Yb	96.3	3.7	0	40.9	59.1
Lu	96.4	3.6	0.6	39.4	60.6

Footnote:

[a] CaO and MgO compositions after Polvé and Maury, Unpublished data.

[b] CaO and MgO compositions after Nicod and Chauvel, Unpublished data.

[c] Determined by ICP-MS (VG Plasma Quad, University of Grenoble). Analytical precision is ±5%.

Figure A

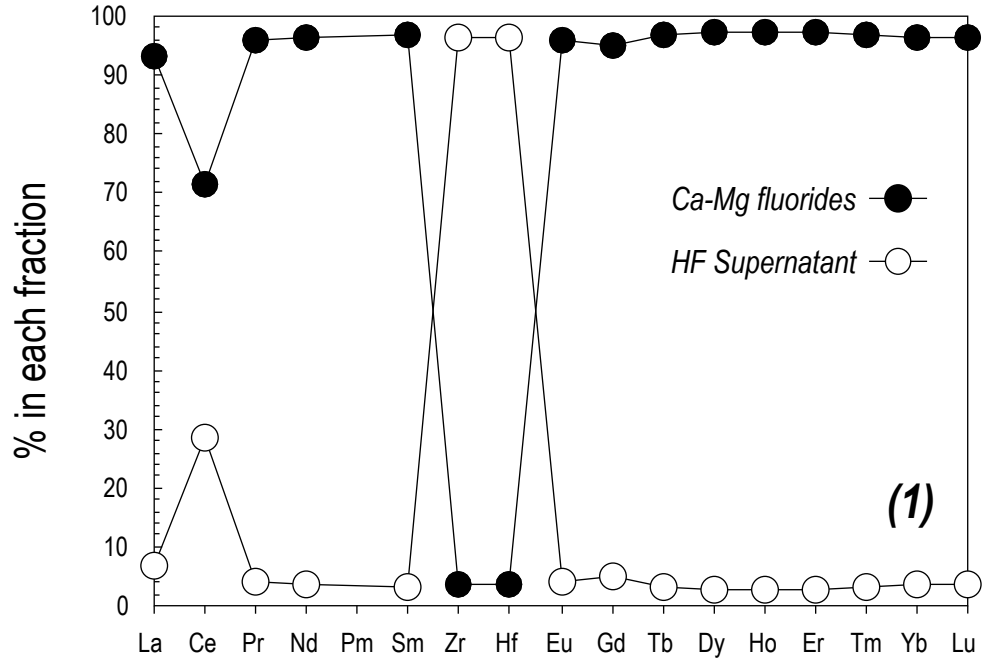
% in each fraction
100
90
80
70
60
50
40
30
20
10
0
La Ce Pr Nd Pm Sm Zr Hf Eu Gd Tb Dy Ho Er Tm Yb Lu
Ca-Mg fluorides
HF Supernatant
(1)

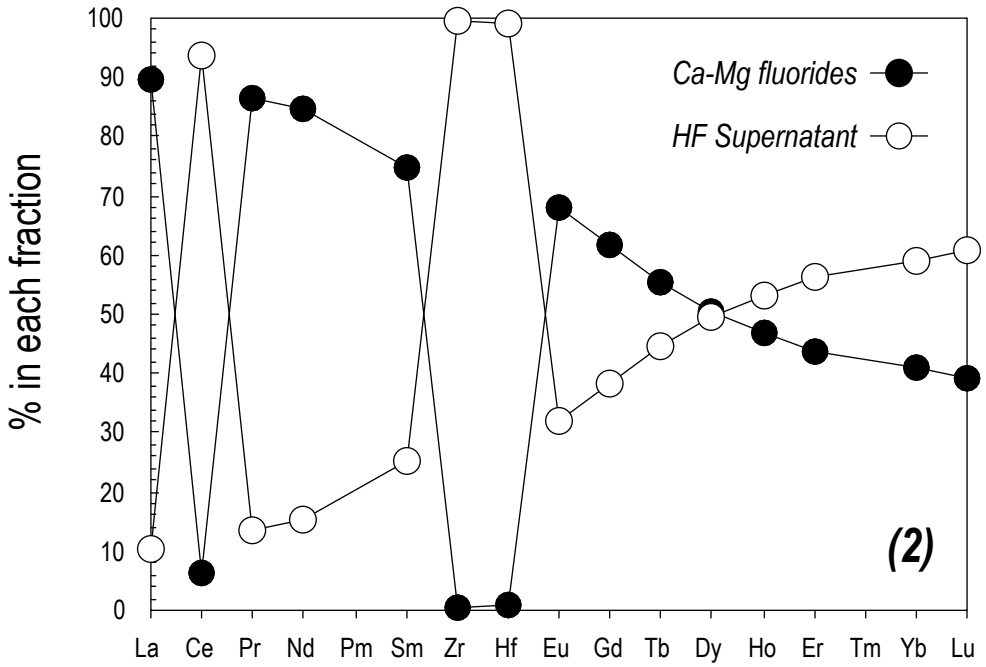
% in each fraction
100
90
80
70
60
50
40
30
20
10
0
La Ce Pr Nd Pm Sm Zr Hf Eu Gd Tb Dy Ho Er Tm Yb Lu
Ca-Mg fluorides
HF Supernatant
(2)

Figure 1

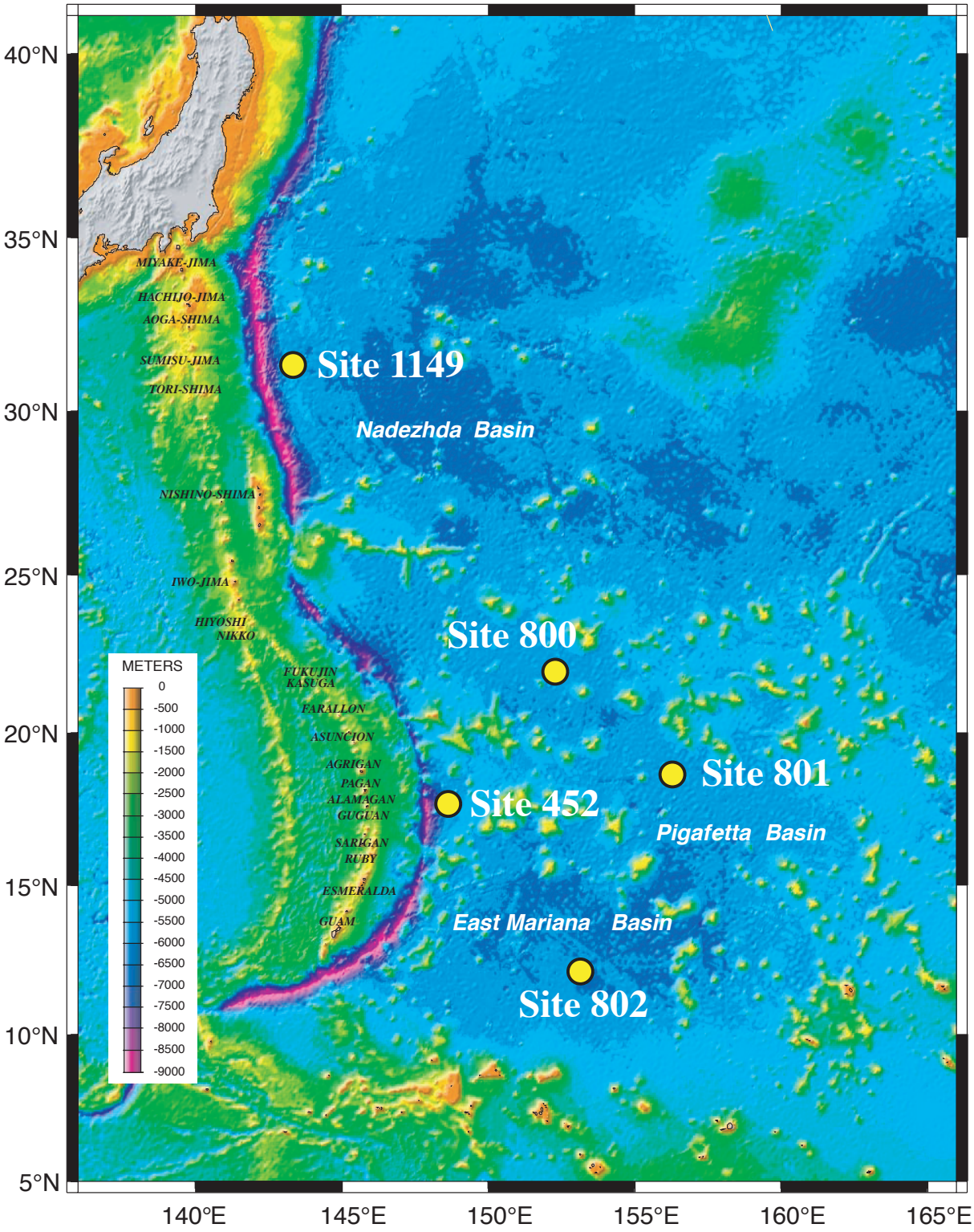
40°N
35°N
30°N
25°N
20°N
15°N
10°N
5°N
140°E
145°E
150°E
155°E
160°E
165°E
METERS
0
-500
-1000
-1500
-2000
-2500
-3000
-3500
-4000
-4500
-5000
-5500
-6000
-6500
-7000
-7500
-8000
-8500
-9000
MIYAKE-JIMA
HACHIJO-JIMA
AOGA-SHIMA
SUMISU-JIMA
TORI-SHIMA
NISHINO-SHIMA
IWO-JIMA
HIYOSHI
NIKKO
FUKUJIN
KASUGA
FARALLON
ASUNCION
AGRIGAN
PAGAN
ALAMAGAN
GUGUAN
SARIGAN
RUBY
ESMERALDA
GUAM
Site 1149
Nadezhda Basin
Site 800
Site 801
Pigafetta Basin
Site 452
East Mariana Basin
Site 802

Figure 2

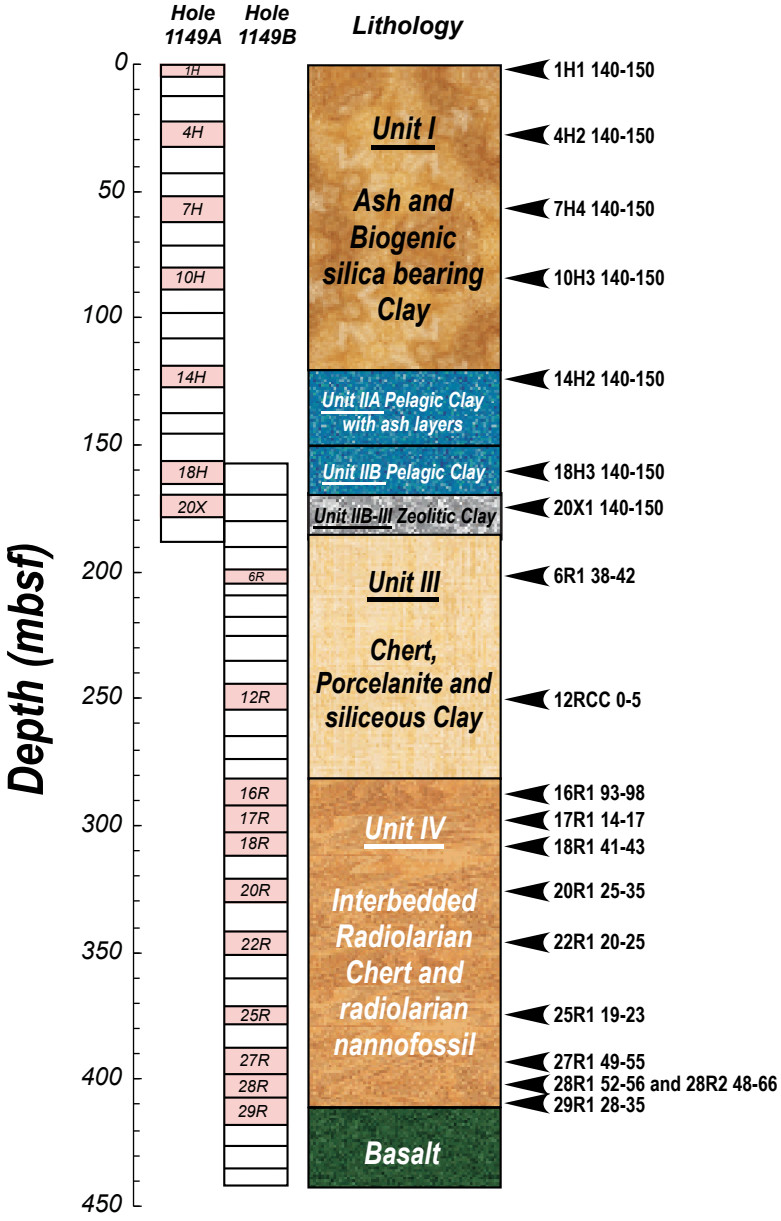
Hole 1149A
Hole 1149B
Lithology
Depth (mbsf)
0
50
100
150
200
250
300
350
400
450
1H
4H
7H
10H
14H
18H
20X
6R
12R
16R
17R
18R
20R
22R
25R
27R
28R
29R
Unit I
Ash and Biogenic silica bearing Clay
Unit IIA Pelagic Clay with ash layers
Unit IIB Pelagic Clay
Unit IIB-III Zeolitic Clay
Unit III
Chert, Porcelanite and siliceous Clay
Unit IV
Interbedded Radiolarian Chert and radiolarian nannofossil
Basalt
1H1 140-150
4H2 140-150
7H4 140-150
10H3 140-150
14H2 140-150
18H3 140-150
20X1 140-150
6R1 38-42
12RCC 0-5
16R1 93-98
17R1 14-17
18R1 41-43
20R1 25-35
22R1 20-25
25R1 19-23
27R1 49-55
28R1 52-56 and 28R2 48-66
29R1 28-35

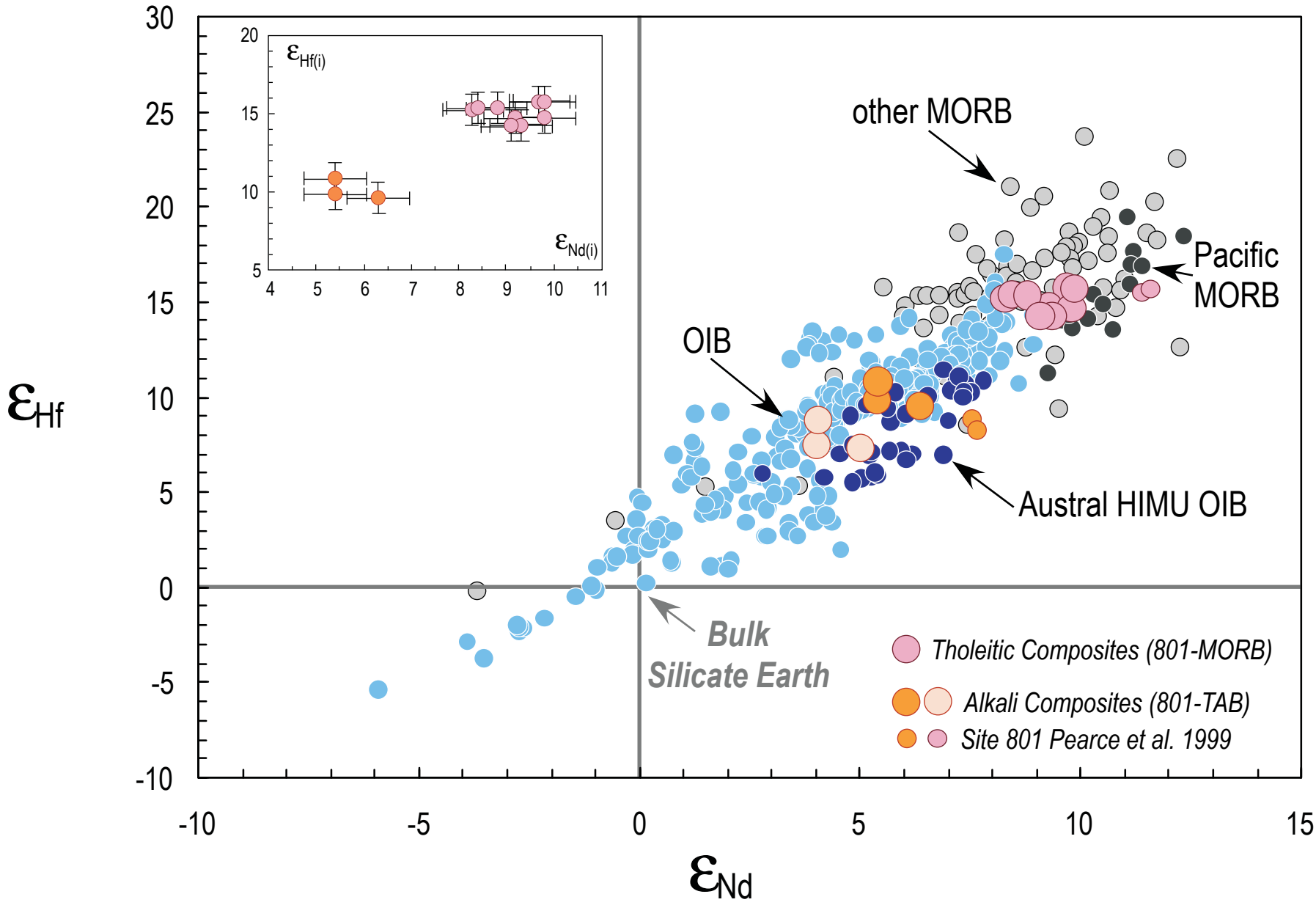
εHf
εNd
30
25
20
15
10
5
0
-5
-10
-10
-5
0
5
10
15
εHf(i)
εNd(i)
20
15
10
5
4
5
6
7
8
9
10
11
other MORB
Pacific
MORB
OIB
Austral HIMU OIB
Bulk
Silicate Earth
Tholeitic Composites (801-MORB)
Alkali Composites (801-TAB)
Site 801 Pearce et al. 1999

Figure 3

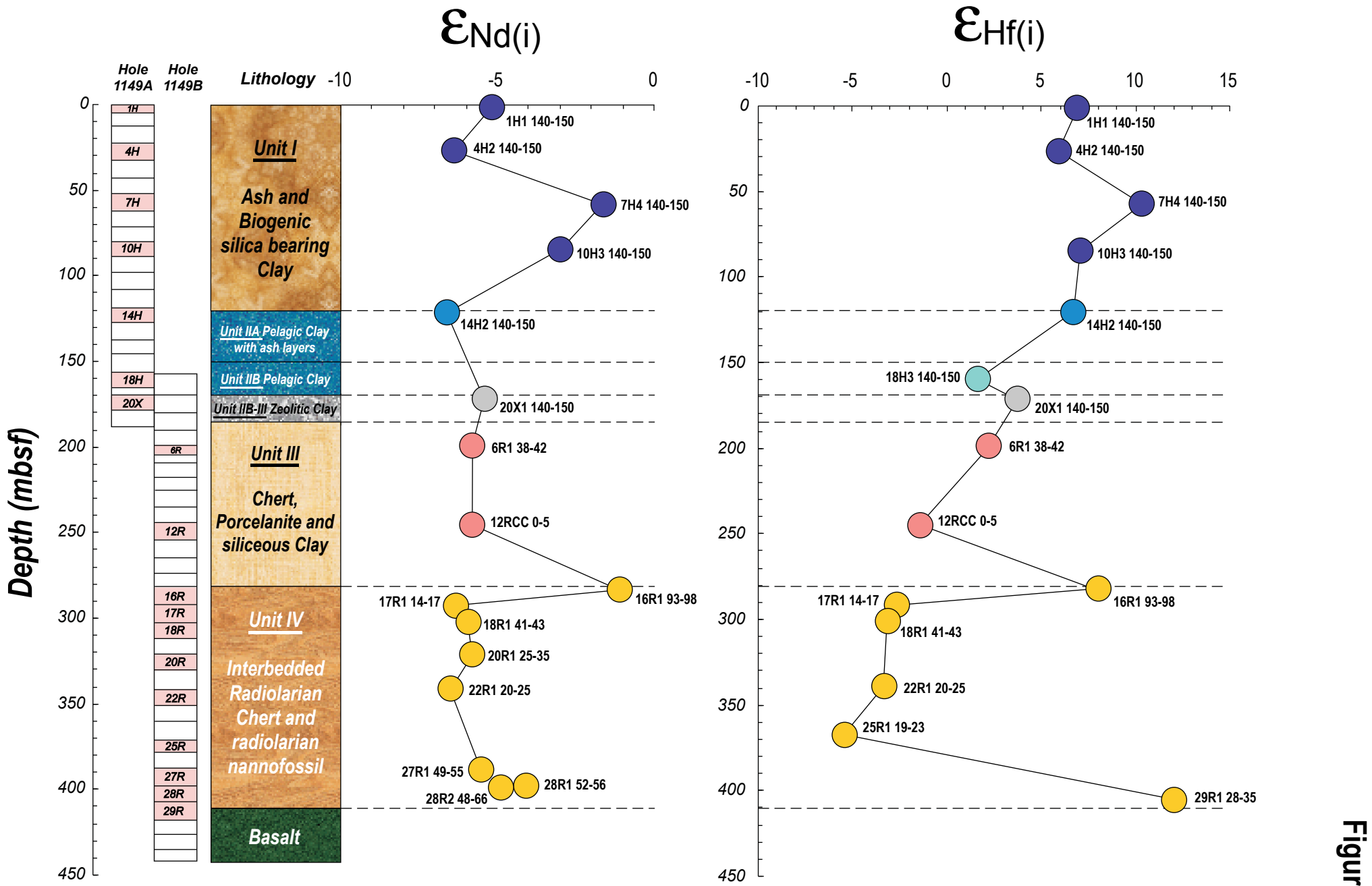
εNd(i)
εHf(i)
Hole 1149A
Hole 1149B
Lithology
Depth (mbsf)
Unit I
Ash and Biogenic silica bearing Clay
Unit IIA Pelagic Clay with ash layers
Unit IIB Pelagic Clay
Unit IIB-III Zeolitic Clay
Unit III
Chert, Porcelanite and siliceous Clay
Unit IV
Interbedded Radiolarian Chert and radiolarian nannofossil
Basalt
1H1 140-150
4H2 140-150
7H4 140-150
10H3 140-150
14H2 140-150
18H3 140-150
20X1 140-150
6R1 38-42
12RCC 0-5
16R1 93-98
17R1 14-17
18R1 41-43
20R1 25-35
22R1 20-25
25R1 19-23
27R1 49-55
28R1 52-56
28R2 48-66
29R1 28-35

Figure 4

Figure 5

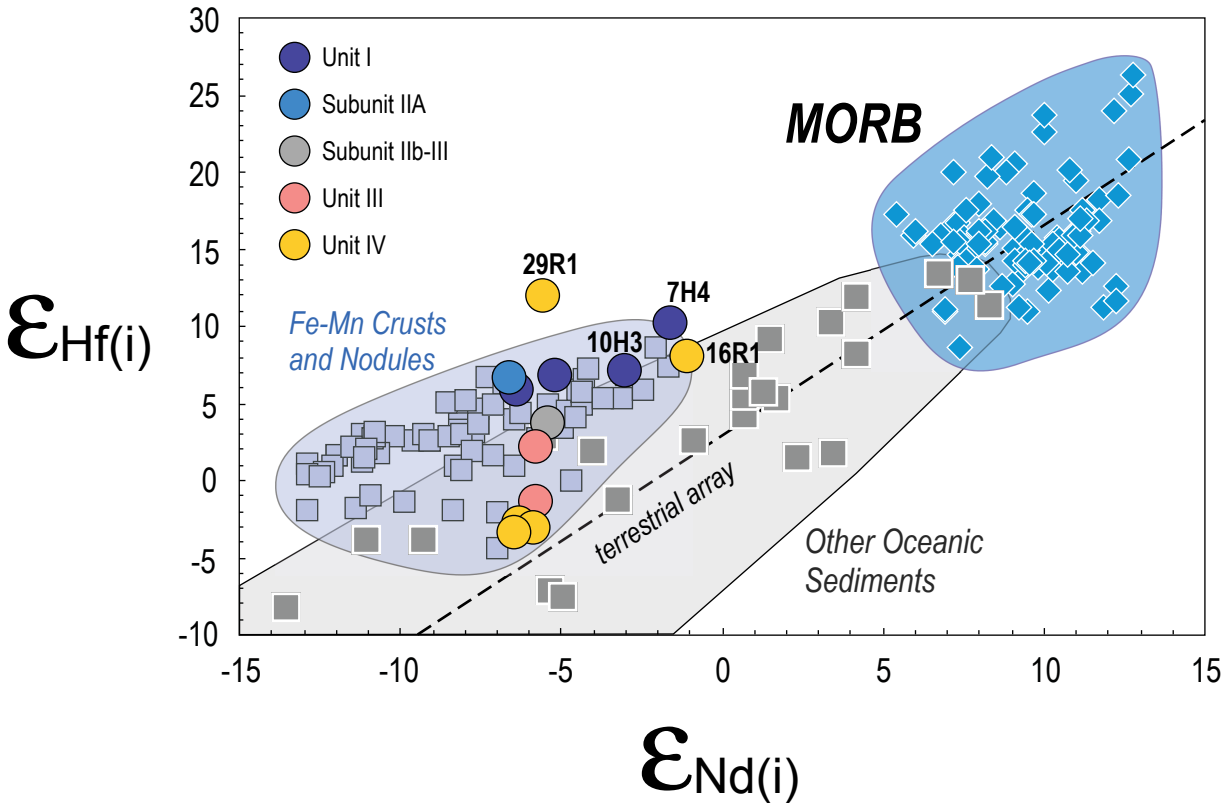
Unit I
Subunit IIA
Subunit IIb-III
Unit III
Unit IV
MORB
29R1
7H4
10H3
16R1
Fe-Mn Crusts
and Nodules
terrestrial array
Other Oceanic
Sediments
30
25
20
15
10
5
0
-5
-10
-15
-10
-5
0
5
10
15
εHf(i)
εNd(i)

Figure 6

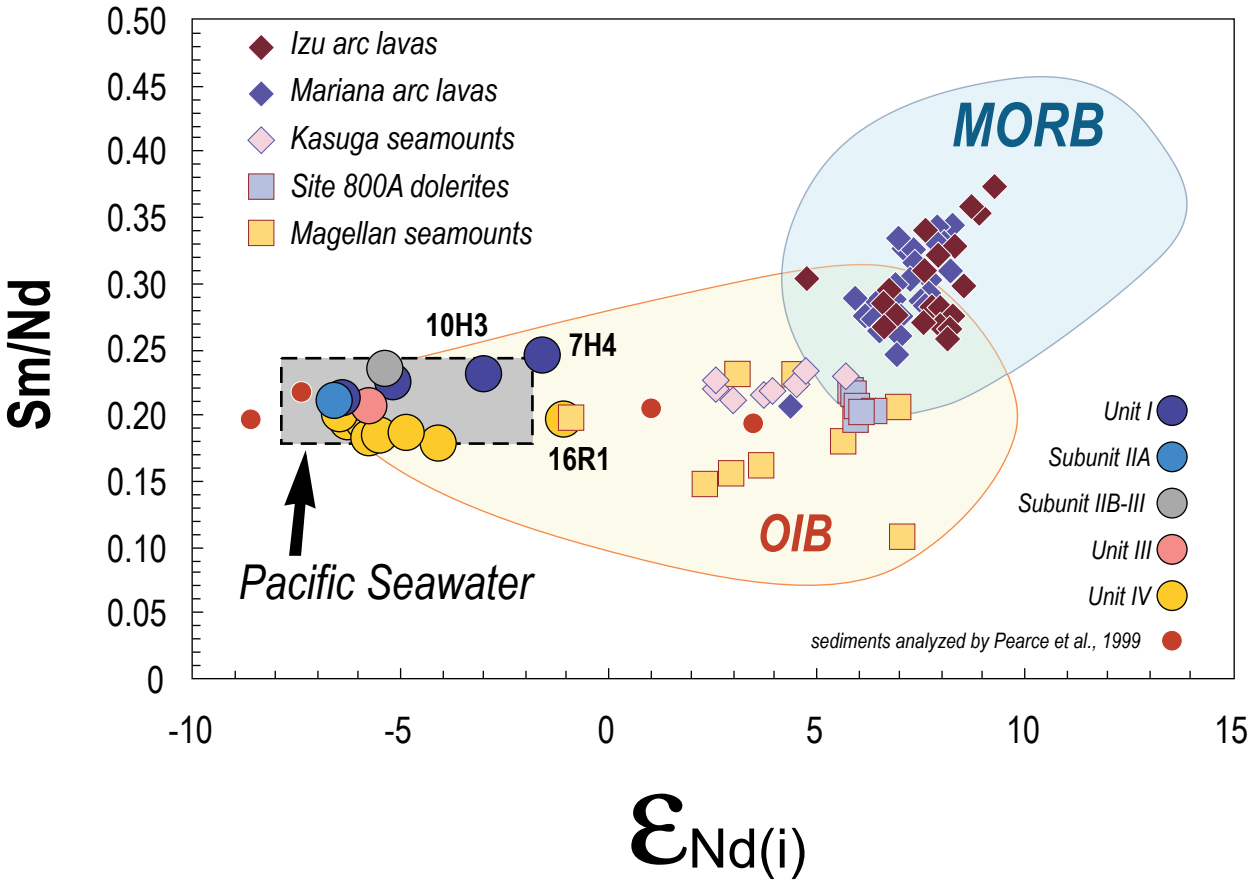
Sm/Nd
0.50
0.45
0.40
0.35
0.30
0.25
0.20
0.15
0.10
0.05
0
-10
-5
0
5
10
15
εNd(i)
Izu arc lavas
Mariana arc lavas
Kasuga seamounts
Site 800A dolerites
Magellan seamounts
MORB
OIB
10H3
7H4
16R1
Pacific Seawater
Unit I
Subunit IIA
Subunit IIB-III
Unit III
Unit IV
sediments analyzed by Pearce et al., 1999

Figure 7

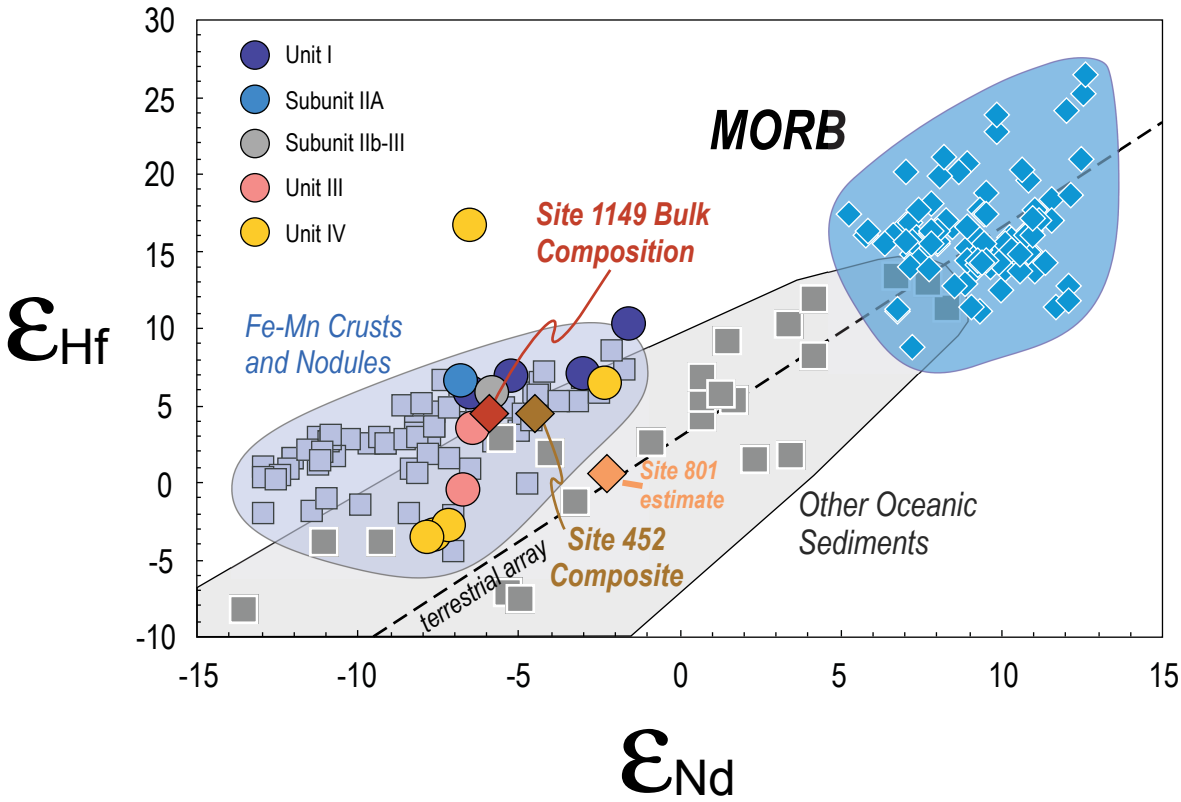
30
25
20
15
10
5
0
-5
-10
-15
-10
-5
0
5
10
15
εHf
εNd
Unit I
Subunit IIA
Subunit IIb-III
Unit III
Unit IV
MORB
Site 1149 Bulk Composition
Fe-Mn Crusts and Nodules
Site 801 estimate
Site 452 Composite
Other Oceanic Sediments
terrestrial array

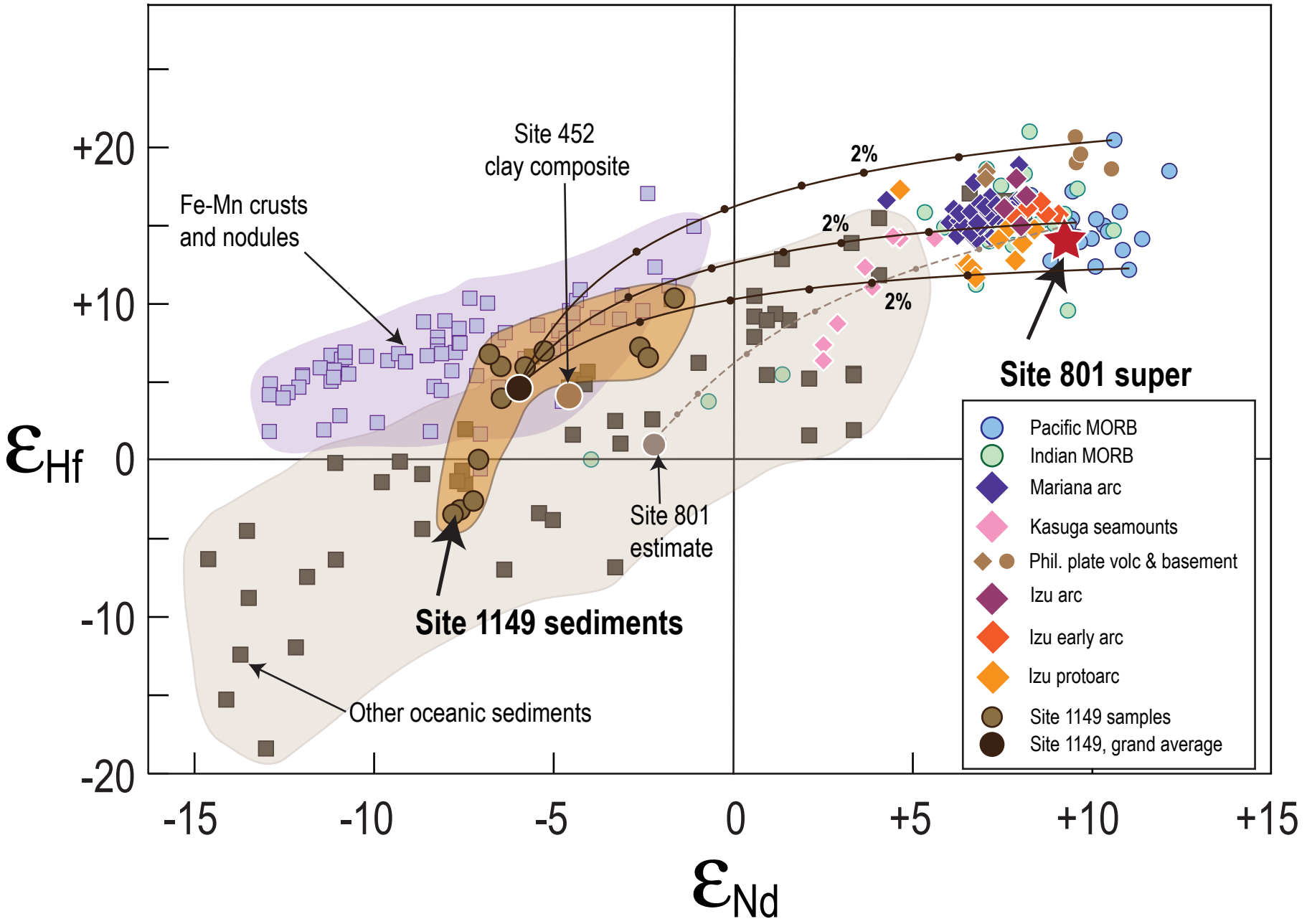
+20
+10
0
-10
-20
εHf
-15
-10
-5
0
+5
+10
+15
εNd
Site 452
clay composite
Fe-Mn crusts
and nodules
2%
2%
2%
Site 801 super
Site 801
estimate
Site 1149 sediments
Other oceanic sediments
Pacific MORB
Indian MORB
Mariana arc
Kasuga seamounts
Phil. plate volc & basement
Izu arc
Izu early arc
Izu protoarc
Site 1149 samples
Site 1149, grand average

Figure 8

Figure 9

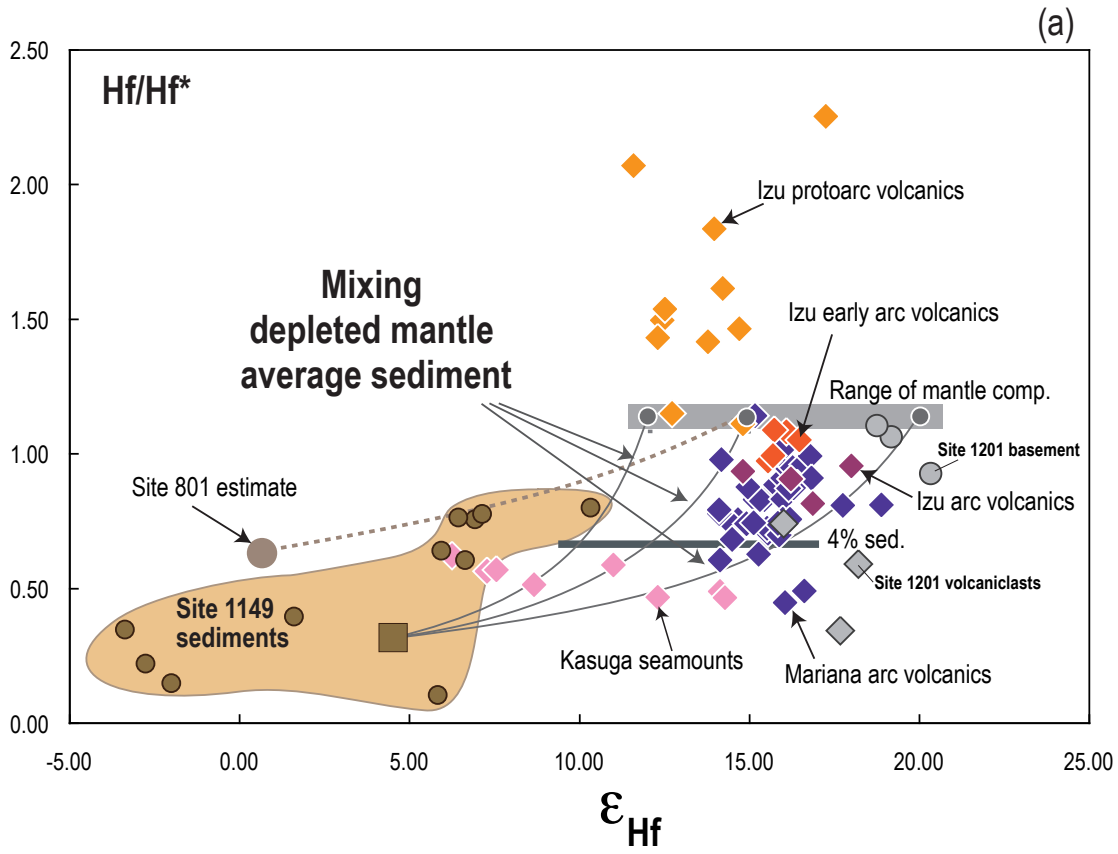
(a)
Hf/Hf*
2.50
2.00
1.50
1.00
0.50
0.00
-5.00
0.00
5.00
10.00
15.00
20.00
25.00
εHf
Mixing
depleted mantle
average sediment
Izu protoarc volcanics
Izu early arc volcanics
Range of mantle comp.
Site 1201 basement
Izu arc volcanics
4% sed.
Site 1201 volcaniclasts
Site 801 estimate
Site 1149
sediments
Kasuga seamounts
Mariana arc volcanics

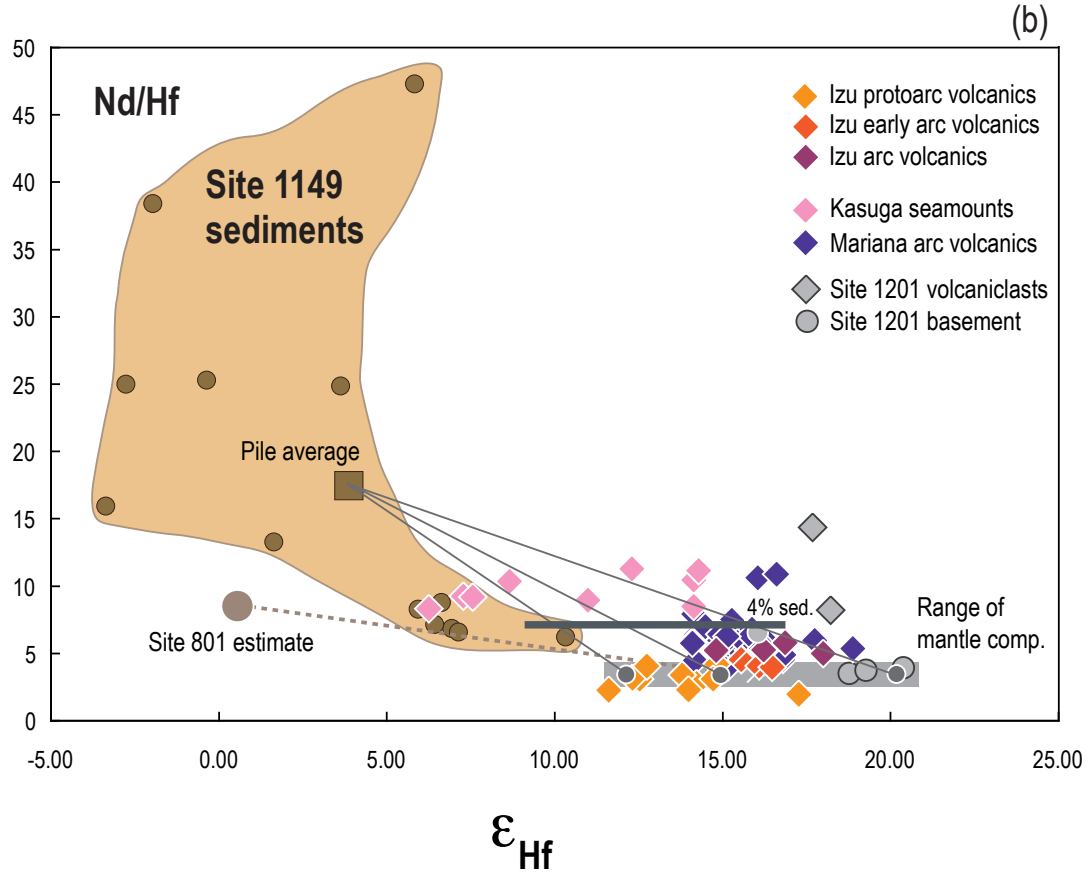
(b)
Nd/Hf
50
45
40
35
30
25
20
15
10
5
0
-5.00
0.00
5.00
10.00
15.00
20.00
25.00
εHf
Site 1149
sediments
Izu protoarc volcanics
Izu early arc volcanics
Izu arc volcanics
Kasuga seamounts
Mariana arc volcanics
Site 1201 volcaniclasts
Site 1201 basement
Pile average
Site 801 estimate
4% sed.
Range of
mantle comp.

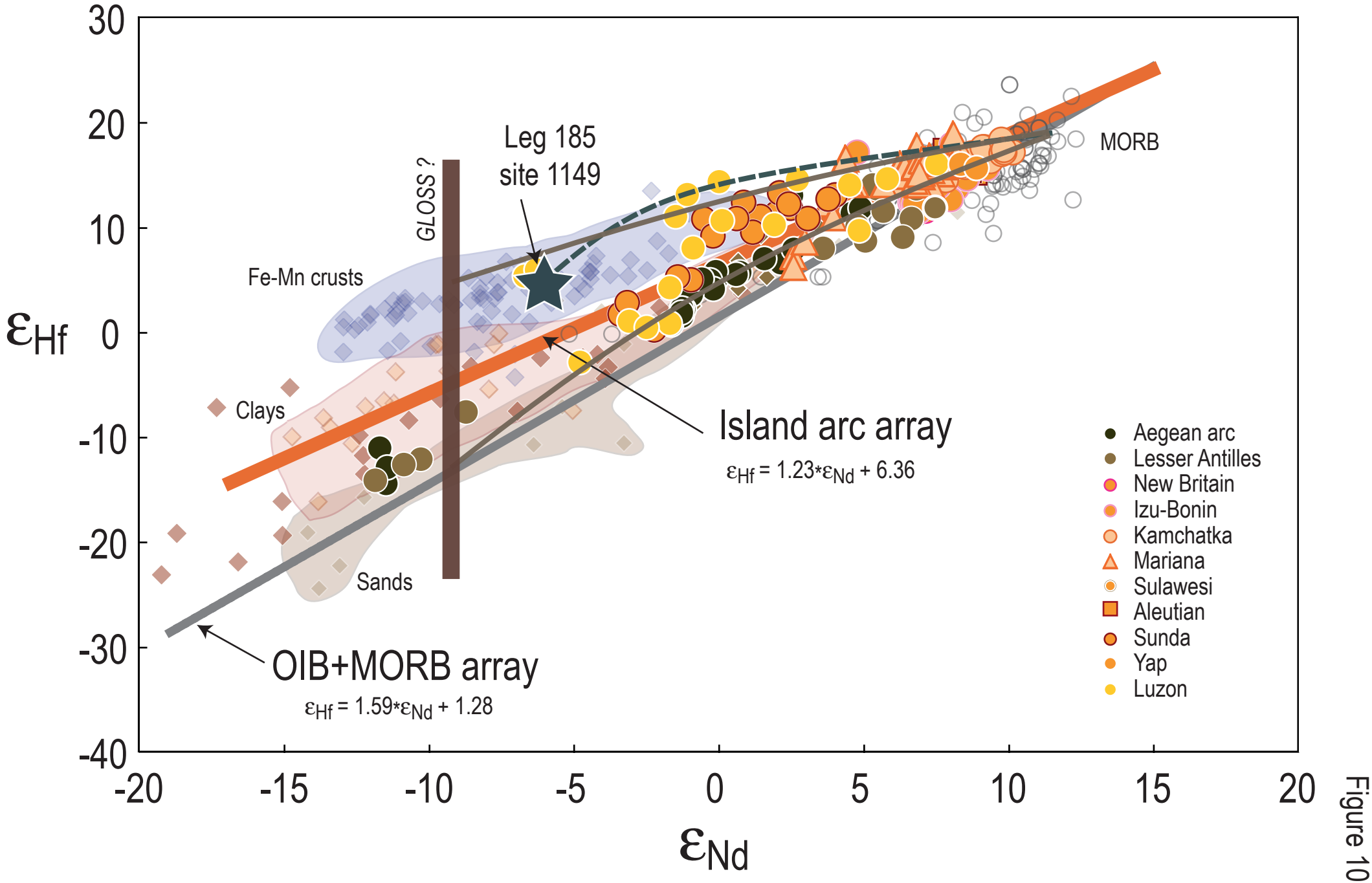
30
20
10
0
-10
-20
-30
-40
-20
-15
-10
-5
0
5
10
15
20
εHf
εNd
Leg 185
site 1149
GLOSS ?
MORB
Fe-Mn crusts
Clays
Sands
Island arc array
εHf = 1.23*εNd + 6.36
OIB+MORB array
εHf = 1.59*εNd + 1.28
Aegean arc
Lesser Antilles
New Britain
Izu-Bonin
Kamchatka
Mariana
Sulawesi
Aleutian
Sunda
Yap
Luzon

Figure 10